

ISSN 2310-6697

otoiser—open transactions on independent scientific-engineering research

# FUNKTECHNIKPLUS # JOURNAL

Théorie—Expérimentation—Métrologie—Logiciel—Applications

ISSUE 37 — SATURDAY 31 MAY 2025 — YEAR 12

Front Cover - Contents

2 About

3 Editorial Group

4 Submissions

4 Download Links

Papers

# Electrical Engineering — Théorie

5 On Ageing of Insulation Materials and Systems:  
Some Thoughts and Comments  
M. G. Danikas

# Telecommunications Engineering — Application

23 The Subtle Details of Combining the Arts of  
Antenna Design, Construction, and Measurement  
- The Radial Discone Paradigm -  
N. I. Yannopoulou and P. E. Zimourtopoulos

Back Cover



About

*This small European Journal is  
In the Defense of Honesty in Science and Ethics in Engineering*

**Period B'**

Previous Period 2013-2024

**Publisher**

otoiser—open transactions on independent scientific  
engineering research

ARG IA0I NFI Lab—Antennas Research Group Informal  
Association Of Individuals No Finance Involved Laboratory  
Scheiblingkirchen, Austria

**Language** — We emphasize the European Origins of our Journal by using English, German and French in its title, as well as, a Hellenic vignette in the front page. However, since we recognize the dominance of US English in the technical literature, we adopted it as the Journal's language.

**Focus** — We consider Radio-FUNK, which still creates a vivid impression of the untouchable, and its Technology-TECHNIK, from an Advanced-PLUS point of view, Plus-PLUS Telecommunications Engineering, Electrical Engineering and Computer Science, that is, we dynamically focus at any related scientific-engineering research regarding Théorie, Expérimentation, Métrologie, Logiciel, ou Applications.

**Scope** — We emphasize the scope broadness by extending the title of the Journal with a Doppelkreuz-Zeichen # which we use as a placeholder for the substitution of its disciplines

**Frequency** — Excluding *forces majeures*, we publish 3 issues per year: on 31st of January, on 31st of May, and on 30th of September.

**Editions** — We increase the edition number of an issue only when is absolutely needed to reform one or more of its papers—thus to increase their version numbers—but we keep unchanged its 1st edition date shown on its front page and we number its pages sequentially from 1. We count the editions of *About* separately.

**Format** — We use a fixed-space font, hyphenation, justification, unfixed word spacing, and the uncommon for Journals A5 (half A4) page size to achieve WYSIWYG printing and clear reading of 2 to 4 side-by-side pages on wide-screen displays.

**Copyright** — We publish under the Creative Commons Attribution CC-BY 3.0 Unported or CC-BY 4.0 International Licenses.

**Editorial Group****# Electrical Engineering**

# High Voltage Engineering # Insulating Materials

Professor Michael Danikas, mdanikas@ee.duth.gr  
EECE, Democritus University of Thrace, Greece

Professor Ramanujam Sarathi, sarathi@ee.iitm.ac.in  
EE, Indian Institute of Technology Madras, India

**# Telecommunications Engineering**

# Antennas # Metrology # EM Software # Simulation # Virtual Labs  
# Applied EM # Education # FLOSS # Amateur Radio # Electronics

Dr. Nikolitsa Yannopoulou, yin@arg.op4.eu \*  
Diploma Eng-EE, MEng-Telecom-EECE, PhD-Eng-Antennas-EECE  
Independent Researcher, Scheiblingkirchen, Austria

Dr. Petros Zimourtopoulos, pez@arg.op4.eu \*  
BSc-Physics, MSc-Radio-Electronics, PhD-Antennas-EE  
Independent Researcher, Scheiblingkirchen, Austria

\* Copy and Layout Editing, Proof Reading, Issue and Website  
Management, Paper and About Reprints, Volumes and Web Pages

**Submissions**

We can only consider papers written in the preferable and recommended odt format of LibreOffice, or even a paper in the MS Office with MathType doc format, if it would be proved that it is fully compatible with LibreOffice indeed.

**Legal Notice** – It is taken for granted that the submitter–correspondent author accepts, without any reservation, the totality of our publication conditions as they are analytically detailed here, in this *About*, as well as, that he also carries, in the case of a paper by multiple authors, the independent will of each one of his co-authors to unreservedly accept all the aforementioned conditions for their paper.

**Electronic Publishing**

We regularly use the Free Libre Open Source Software Libre Office with the Free Liberation Mono font and the Freewares PDFCreator and PDF-Xchange Viewer. We also use some basic html code of ours and the Free Open Digital Library of Internet Archive website, where we upload the FTP#J Collection of Issues, Paper reprints, *About* documents, and Volumes, in both portrait and landscape orientations, for download or very clear online reading with the Free Open Source BookReader.

**Internet Addresses**

**Submissions** : sub@ftpj.otoiser.org

**Send Updates** : updates@ftpj.otoiser.org

**Paper Template** : <https://www.template.ftpj.otoiser.org>

**Reference Updates** : <https://www.updates.ftpj.otoiser.org>

**Internet Publishing** : <https://www.ftpj.otoiser.org>

**The FTP#J Collection at Internet Archive Digital Library** :  
<https://archive.org/details/@funktechnikplusjournal>

Please download the latest *About* edition from  
<https://about.ftpj.otoiser.org>

*This document is licensed under a Creative Commons Attribution 4.0 International License – <https://creativecommons.org/licenses/by/4.0>*

# On Ageing of Insulation Materials and Systems: Some Thoughts and Comments

M. G. Danikas

Democritus University of Thrace, Department of Electrical and Computer Engineering, 67100 Xanthi, Greece

## Abstract

Ageing has been and still is one of the major - if not the major - challenges regarding insulation systems and materials. The present paper goes through a brief description of some fundamental models of ageing and points out aspects that deserve to be further investigated. Factors that affect (or may affect) the ageing of insulations are discussed.

## Keywords

Insulation ageing, multi-factor ageing, electrical stress, thermal stress, enclosed cavity, enclosed void, partial discharges, inception voltage, extinction voltage, ignition event, Arrhenius equation

## Introduction

Ageing is something that humans want to avoid discussing whereas insulation experts tend to intensively research this subject. A most distinguished expert on ageing, the late E. L. Brancato wrote once that "the phenomenon of ageing is one that mankind prefer to ignore while industry prefers to explore". Ageing of insulation materials or insulation systems can come about either from a single deteriorating factor (e.g. electrical stress,

mechanical stress or temperature rise) or from a multiplicity of factors, such as e.g. a combined electrical and thermal stressing or electrical stressing and humidity. As was noted in [1], ageing may induce changes in the material itself that are bound to affect a property (or properties) of the material. Consequently, when a property falls below a certain value, breakdown may ensue. Such a type of ageing may be characterized as intrinsic. A polymer that deteriorates and its

electric strength or tensile strength falls below a certain critical value, is an example of such an intrinsic failure. On the other hand, ageing may be also affected by changes in the presence of asperities on the electrodes, foreign particles or defects that may come about during the preparation of a material or an insulation system. Such defects may inadvertently influence a property or properties of the insulation leading to a catastrophic failure. This type of deterioration is an example of extrinsic ageing. Intimately related to the notion of ageing are the proposed models for the prediction of insulation lifetime. Acceleration tests (by enhancing either the electrical stress or the frequency applied and then extrapolating to find the expected real lifetime of an insulation system) have been conceived by a large number of researchers and the analysis of ageing data has been the subject of a large number of publications over a number of decades. In this paper, a brief review will be given on some of the proposed models together with comments on both the ageing of insulation systems and also on what we call "prediction of insulation lifetime".

## The notion of ageing and some proposed models

According to IEC TC 63 [2], ageing is the "irreversible deleterious change to the serviceability of insulation systems. Such changes are characterized by a failure rate which increases with time". Put it another way, ageing is properties changing with time or the response of the insulation to various stress factors [3].

One may distinguish several forms of ageing, namely, thermal, electrical, environmental and mechanical. Thermal ageing is associated with thermally activated chemical processes. It was Dakin who indicated that since the physical changes in an insulating material are the result of internal chemical changes, the theory of chemical reaction rates may be applied to analyze data on ageing [4]. He considered that the instantaneous rate of change of the number of molecules undergoing a transformation with time is proportional to the number present raised by some exponent, i.e.

$$dC/dt = -KC^n \quad (1)$$

where, C the variable number per unit volume or concentration, K the rate constant and n the exponent determining the order of the reaction. By

integrating (1) and by taking  $n=1$ , the following equation ensues,

$$\log_e C = -Kt + \log_e C_0 \quad (2)$$

and

$$C = e^{-Kt} C_0 \quad (3)$$

A mathematical function of the concentration of the most important chemical constituent can be found which is an integral of (1), regardless of what the order of the reaction is or whether the rate constant varies with time, i.e.

$$f_0(C) = -K_0 t \quad (4)$$

where,  $K_0$  the rate constant is time independent and dependent on temperature.

By introducing the assumed relation between the physical property and the concentration of the most significant chemical constituent given in (5),

$$P = f(C) \quad (5)$$

( $P$  being the magnitude of the physical property which is of interest and  $C$  the concentration of an important chemical constituent of the insulation which is being changed by the thermal ageing), a simple relation between the physical property and time may be obtained, i.e.

$$f_0'(P) = -K_0 t \quad (6)$$

If the temperature dependence of a reaction rate is given by

$$K_0 = A e^{-B/T} \quad (7)$$

it follows that

$$f_0'(P)/t = K_0 = A e^{-B/T} \quad (8)$$

with  $A$  and  $B$  constants and  $T$  the absolute temperature. Evidently, as follows from (8), the logarithm of the time to reach a particular value of a certain property of the insulation is proportional to the reciprocal of the absolute temperature and from (6) and (7) one may conclude that each magnitude of a physical property corresponds to a particular concentration of the significant chemical constituents, this concentration being the same for the same magnitude of the physical property no matter if it is attained at high or low temperatures.

A model proposed by Allen and Tustin in [5] was based on Guldberg and Waage's law of mass action

$$[d(n_0 - n)]/dt = Kn \quad (9)$$

where,  $K$  is the velocity coefficient for the chemical process,  $n_0$  is the number of molecules involved in the chemical process causing change in the critical property and  $n$  is the number of unchanged molecules. Eq. (9) written differently gives

$$dn/n = -A \exp(-E/RT) dt \quad (10)$$

with  $A$  a constant,  $E$  the activation energy for the reaction,  $R$  the gas constant,  $T$  the absolute temperature and  $n$  as above. If time to failure is  $t_f$  at constant absolute temperature  $T$  with  $n_f$  and  $n_0$  being the unchanged molecules and the original number of molecules respectively, by integrating (10), we have that

$$\ln(n_f/n_0) = -A \exp(-E/RT)t_f \quad (11)$$

from which it follows that

$$\ln[\ln(n_f/n_0)] = \ln t_f + \ln A - (E/RT) \quad (12)$$

The latter equation - assuming that the material behaves consistently -,  $n_f/n_0$  is the same for each failure and finally (12) is transformed to

$$\ln t_f = C + B/T \quad (13)$$

The approach of [5] is not that different from Dakin's approach since the inverse of the absolute temperature is again involved. The weak point of these approaches is that they consider that there is a main chemical reaction taking place in the insulation whereas there may take place more chemical reactions.

Electrical ageing may be due to several reasons, such as partial discharges from asperities of the electrodes and/or microcavities as well as from charge injection owing to exceedingly high electric field enhancements. As the electrical stress increases, the lifetime of an insulation may decrease. The well known inverse power law may be expressed as

$$L = k V^{-n} \quad (14)$$

with  $V$  the applied voltage and  $k$  a constant,  $n$  being the power law constant [6]. Other models that were developed did not radically differ from the model of (14) [7], [8]. It must be emphasized that the electrical ageing equations are empirical and not developed by way of expressions for the reaction rate, as was noted in [3].

The environmental stress may include the influence of humidity, radiation, pressure and temperature. The environ-

ment in which take place the various effects (such as oxidation) will certainly affect the chemical reactions that may influence the deterioration of the insulation. Environmental stressing is evident in outdoor insulating systems but it is not necessarily confined there.

Mechanical ageing may come about from structural defects, such as microcracks and microcavities. Different thermal expansion coefficients may cause delamination in electrical machines insulation and thus lead to the rise of partial discharges and eventually to a catastrophic failure. Furthermore, mechanical stressing (either internal or external) may influence the development and propagation of electrical trees, in other words mechanical stresses tend to affect in a crucial manner the inner workings of an insulation, providing thus paths to breakdown [9].

#### **The notion of multi-factor ageing**

The difficulty with multi-factor ageing is that more than one (or usually two) factors act simultaneously on the insulation. Simultaneous ageing by more than one factors means that there may be interaction between these factors. According to [10], direct interaction is an "in-

teraction between simultaneous applied factors of influence, which differs from that occurring with sequentially applied factors of influence. Factors producing direct interaction are not necessarily ageing factors" whereas indirect interaction is an "interaction between simultaneous applied factors of influence, which remains essentially unchanged when the factors are applied sequentially. Indirect interaction can only be caused by ageing factors" [10].

A most common type of multi-factor stressing is the combined thermal-electrical stressing. Two models appropriate for two different types of insulating materials have been developed for such a combined stressing: (1) for those when stressed below a certain value of electrical stress, life tends to become infinite and (2) for those showing an ever decreasing life even for very long test times [11], [12]. These models can be expressed in terms of the Arrhenius equation, the inverse power law and the threshold equation, the latter describing the electrical behavior of materials which below a certain value of electrical stress do not show any signs of electrical ageing. Simoni, the author of [11], [12], considered that type

(1) materials can be expressed in terms of the Arrhenius equation and the threshold equation and that type (2) materials can be expressed in terms of the Arrhenius equation and the inverse power law. In yet another publication [13], the authors, confronted with the problem of how to combine the results of life tests involving temperature and voltage separately so as to evaluate the life at the combined operating stresses, observed that (a) at room temperature, a limited but significant reduction in breakdown voltage may be noticed, (b) at high temperatures the decrease in breakdown voltage due to electrical stress is larger than at room temperature and more significant as the temperature increases, and (c) the total decrease in breakdown voltage observed when the two stresses are simultaneously applied is substantially larger than the sum of the decreases observed for each factor acting alone. This is a good example of a synergy of the ageing factors. Very similar views were also expressed earlier [14].

#### **Short presentation and evaluation of some existing multi-factor ageing models**

Simoni's model [11], [12], [15] - [17] assumes that for

a given insulation system the time to breakdown with a combination of electrical and thermal stresses can be reduced to finding a resultant ageing rate [3], that is

$$R(T, E) = A \exp(-B/T) \exp((\alpha + b/T) f(E)) \quad (15)$$

where,  $R(T, E)$  is the reaction rate,  $A$  and  $B$  are constants,  $T$  and  $E$  the absolute temperature and the electric stress respectively,  $\alpha$  and  $b$  constants under the combined stress and  $f(E)$  an unspecified function of electrical stress [3]. It goes without saying that since the reaction rate is inversely proportional to the absolute temperature, the expected time to breakdown  $L(T, E)$  will be expressed in terms of a reference expected lifetime  $L_0$ , i.e.

$$L(T, E) = L_0 \exp[-B \Delta(1/T)] (E/E_0)^{-N} \quad (16)$$

with  $B$  a constant,  $E_0$  a reference electric stress for electrical ageing,  $\Delta(1/T) = 1/T_0 - 1/T$ ,  $T_0$  being the room temperature and  $N$  denoting the thermal synergism.

Ramu's model [18], [19] can be described by the following equation, where  $L(T, E)$  the time to breakdown and the

various  $c$  and  $n$  parameters are dependent on temperature,

$$L(T, E) = \exp[c_1 - c_2 \Delta(1/T)] E^\lambda \exp(-B\Delta(1/T)) \quad (17)$$

with  $\lambda = [-n_1 - n_2 \Delta(1/T)]$ , or in terms of a reference time to breakdown  $L_0$  and a reference electric stress  $E_0$ ,

$$L(T, E) = L_0 (E^{n_2} \Delta(1/T)/E_0)^{-n_1} \exp(-B \Delta(1/T)) \quad (18)$$

Ramu assumed that  $L_0$  is the time-to-breakdown at room temperature and  $E_0$  is the operating stress.

Fallou's model [13], [20] consists of an equation which relates the time-to-breakdown  $L$  with electrical stress related functions  $A(E)$  and  $B(E)$  [3],

$$L = \exp[A(E) + B(E)/T] \quad (19)$$

with  $A(E) = A_1 + A_2 E$  and  $B(E) = B_1 + B_2 E$ ,  $A_1$ ,  $A_2$ ,  $B_1$ ,  $B_2$  being constants determined experimentally from time-to-breakdown curves at constant temperatures [3].

The basic comment on the above very briefly described models - taking into account the combined electrical and thermal stresses - is that all of them are based on Dakin's approach and on the inverse power law. All of the

aforementioned models seem to be semi-empirical. Dakin's approach in turn was also based on an earlier model proposed by Eyring, which described changes in the rate of a chemical reaction with temperature [21]. This is not to be taken as criticism of the above models since they contributed immensely to our understanding of the interplay between electrical and thermal stresses.

#### **Gjaerde's approach on multi-factor ageing**

An interesting study carried out in the context of a Ph.D. thesis indicated that for epoxy resin samples ageing, a critical parameter is the pressure inside an enclosed cavity [3]. It has been shown that a large cavity pressure reduction rate is accompanied by a short time-to-breakdown whereas a small cavity pressure reduction leads to a longer time-to-breakdown. Gjaerde's model assumes that there is an electrical threshold below which no electrical ageing takes place. This is an assumption taken into account by many researchers. However, in [3], Gjaerde draws attention to the fact that cavity pressure variations are strongly related to partial discharge (PD) patterns. Partial discharges in turn appear in

different forms and mechanisms and thus very small discharges may go undetected. In [3], it is rightly discussed that light emission of discharges may be a much more sensitive detection means than their electrical detection and, consequently, swarming pulsive micro-discharges may evade detection by conventional detection systems. Gjaerde rightly writes that "drawing conclusions from an incomplete PD pattern, i.e. a pattern which does not include all PD types, may very well be impossible".

The inability of conventional PD detection systems to register very small PD, and indeed the possible charging effects below the so-called inception voltage were discussed in length, among others, in [22] - [30]. Not to be discarded is also the role of space charge effects on the lifetime of an insulation and their intimate relationship with the gas conductivity inside an enclosed cavity [31]. As was explained in [31], charging phenomena and ionization processes of low energy may occur, implying thus that charges appearing in the cavity may result in clusters of space charges on the cavity walls. Such a space charge results in an electric field which - in the case of AC fields - is added

to the applied electric field on the insulation [32]. Things are further complicated since charge packets may cause local chain re-arrangements in polymeric insulation [33].

Gjaerde's approach on ageing strongly reminds us of the importance of exact measurements regarding the partial discharges as well as their respective mechanisms. Reference [3] emphasizes the fact that incomplete PD patterns may yield incomplete information as to the degree of ageing of an insulation. Furthermore, reference [3] also indirectly points out to the importance of distinguishing between inception voltage and ignition voltage, i.e. the importance of differentiating between these two notions. Ignition is not to be considered as harmless. It is not to be forgotten that among the first to stress the difference between ignition and inception was a classical monograph by A. Kelen almost 60 years ago [34].

Consequently, since PD is one of the main causes of insulation failure, it is imperative to realize how significant is to understand what we really measure and to distinguish between the various mechanisms of PD. Older and more recent research can be of great help in clarifying means of the measurement and

mechanisms of PD [35] - [43]. Furthermore, as was remarked in [44], intimately related to the above is the development of techniques to determine temperature rise of cavity surfaces due to PD. As was conjectured in [23], [24], [45], [46], electrical ageing may in fact be a chemical reaction in cavities induced by the deposition of energy. Such deposition may be expended in raising of the temperature of the cavity walls, in delivering gases which possibly will oxidize the cavity walls, which in turn may deteriorate and cause mechanical erosion [44]. The gist of [44] consists in pointing out that "... if a measurement of the joule heating of voids can be obtained, it may make possible that the Arrhenius relations could be employed at a void level".

Gjaerde's approach is remarkable in that it pointed out the importance of what was going on inside the enclosed cavities, the variation of gas pressure and its relation to the ageing of the insulating material. Such an approach agrees with the research done by Bruning and colleagues (mentioned above) as well as with the work carried out earlier, in which it was recommended that "... an adequate understanding of the physics and chemistry of age-

ing be acquired ..." and that "... more sensitive techniques be explored ... at assessing the rate of aging close to operating temperature ..." [47].

#### **Where does all the above lead?**

Certainly, modeling the combined electrical and thermal stressing helps us to try to understand - at least partially - its workings. It goes without saying that Gjaerde's approach also helps us to realize how important is the variation of gas pressure inside enclosed cavities. The deleterious role of PD on insulation ageing is also rightly stressed. All this is well related to PD diagnostics. Earlier research, however, showed that conventional discharge detection techniques do not generally respond to all types of PD and they can yield an indication that may not be completely representative of the total discharge intensity. The magnitude of the small pulses present in the pseudoglow discharge may not be large enough to trigger conventional discharge detectors. Moreover, a number of large pulses (spark-type PD) can actuate the PD detector but the resulting detected discharge pattern will not necessarily contain all the information and consequently will not constitute a true

replica of the actual discharge pulse density distribution. On the other hand, the fact that true pulse discharges do occur simultaneously (even under the appearance of true glow and pseudoglow discharges in innumerable instances) is a remedy for the conventional PD detectors since they permit the determination of the discharge inception and extinction voltages, defined as the voltages at which the apparent charge transfer exceeds or falls below a specific value [48] - [50]. The latter statement, however, ignores the fact that there is a difference between inception and ignition events [34].

There are, however, some further limitations of the PD diagnostics. Even though well established techniques were successful in increasing sensitivity, diminishing noise etc., PD diagnostic techniques have some limitations. As was pointed out in an earlier publication, "... [PD diagnostics] cannot tell anything about those parts of a test object which are not sufficiently stressed to produce PD ... [furthermore] PD diagnostics produce information on the current state of an object's electrical insulation but this does not enable an assessment of its remaining life for the simple

reason that life depends both on the state of a gradually deteriorating object and on the stresses that act on it later" [51], [52].

Another point in need of consideration is that ageing is often more complex than a gradual advance of a single process. As was reported [34], [53], [54], a chain of events in a generator stator insulation was that first there was an increased temperature in a slot insulation of wrapped shellac-bonded paper backed mica splittings with the ensuing delamination and PD activity. Organic components degraded and vibrational forces gradually produced strand movement resulting in abrasion of some mica sheets, grinding into the slot insulation wall and finally in electrical breakdown. This is a good example of PD diagnostics that yield information on mechanisms other than strictly electrical ageing (in this case thermal and mechanical).

Yet another point that must be stressed - although we referred to it before - is that of charging events prior to partial discharges [23], [24], [45]. Previous research also indicated that pulses from water tree regions in polyethylene, as low as 1.2 fC, could be reliably measured [55], [56]. The work of [55], [56] was favorably discussed

by Morel and co-workers in [57]. The latter researchers, in agreement with [55], [56], concluded that signals can be measured many minutes prior to the visual appearance of electrical trees and that there is an "induction" period where no trees are observed. Part of the problematic of the interplay between electrical and water trees was also reported in [58], where it was noted that "... some water trees convert to electrical trees and some do not. ... Is there something in the vicinity of a water tree which undergoes the conversion that is important and that could be detected before the conversion takes place? ... It was mentioned that after the water tree converts to an electrical tree many pulses were required to cause insulation breakdown. The actual number of pulses depended on their type, e.g. lightning, switching surges or single cycles of 60 Hz". As was remarked before, water trees may be in close proximity to "virgin" polymeric material. Consequently, there is a possibility that charging events and/or non-destructive current pulses may somehow slowly degrade the insulation. Such charging events - as reported - may be in the fC range and may lead to chemical changes [23], [24], [45], [55], [56],

[59], [60], [61].

Things become even more complicated when one has to deal not only with insulating materials but also with solid/liquid insulating systems [1]. In the latter case, both weak links existing either in the liquid volume or on the electrode surfaces and physical size factors (such as liquid flow in the gap, stored electrostatic energy in the neighborhood of the gap, inability to reproduce the small system quality in a large system closer to industrial practice) may affect the dielectric strength and consequently the rate of ageing [62].

### Conclusion

In the context of this incomplete review, several issues regarding the ageing of insulating materials and systems were discussed. All reported models have their own particular merits. Gjaerde's approach - pointing out the variation of gas pressure inside enclosed cavities and in fact using already known parameters - seems to be particularly interesting. It remains to be seen, however, whether her approach may be used in larger insulating systems. Some factors - complicating even further - the questions surrounding ageing have been pointed out and discussed.

### References

- [1] Densley J., Bartnikas R., Bernstein B. S., "Multi-stress ageing of extruded insulation systems for transmission cables", IEEE Electrical Insulation Magazine, Vol. 9, No. 1, 1993, pp. 15 - 17
- [2] IEC Report, Publication 505, "Guide for evaluation and identification of insulation systems of electrical equipment", 1975
- [3] Gjaerde A., C., "Multifactor ageing of epoxy - The combined effect of temperature and partial discharges", Ph.D. Thesis, Norwegian University of Science and Technology, Trondheim, Norway, 1994
- [4] Dakin T.W., "Electrical insulation deterioration treated as a chemical rate phenomenon", AIEE Transactions, Vol. 67, Pt. I, 1948, pp. 113 - 122
- [5] Allen P. H. G., Tustin A., "The ageing process in electrical insulation: A tutorial summary", IEEE Transactions on Electrical Insulation, Vol. 7, No. 3, 1972, pp. 153 - 157
- [6] Stone G. S., Kurtz M., Van Heeswijk R.G., "The statistical analysis of a high voltage endurance test on an epoxy", IEEE Transactions on Electrical Insulation, Vol. 14, No. 6, 1979, pp. 315 - 326
- [7] Wasilenko E., "A new approach to needle test of polyethylene", Proceedings of the 3rd International Conference on Dielectric materials, measurements and Applications, Birmingham, UK, 10-13 September 1979, pp. 225 - 226, IEE Conference Publication No. 177
- [8] Makio Y., "The lifetime estimation of plastic films by measuring the specimen temperature rise", Proceedings of the 3rd International Conference on Dielectric materials, measurements and Applications, Birmingham, UK, 10-13 September 1979, pp. 93 - 96, IEE Conference Publication No. 177
- [9] Danikas M. G., Papadopoulos D., Morsalin S., "Propagation of electrical trees under the influence of mechanical stresses: A short review", Engineering, Technology & Applied Research, Vol. 9, No. 1, 2019, pp. 3750 - 3756

- [10] IEC Report Publication 792-1, "The multi-factor functional testing of electrical insulation systems - Part 1: Test procedures", Geneva, Switzerland, 1985
- [11] Simoni L., "Life models of insulating materials for combined thermal-electrical stress", Colloquium on "Ageing of insulating materials under electrical and thermal stresses", London, UK, 1st December 1980, Digest No. 1980/72, pp. 1.1 - 1.9
- [12] Simoni L., "On compatibility between thermal and electrical stress", IEEE Transactions on Electrical Insulation, Vol. 17, No. 4, 1982, pp. 373 - 375
- [13] Fallou B., Burguiere C., "Electrical ageing of insulation combined effect of electrical and thermal stresses", Colloquium on "Ageing of insulating materials under electrical and thermal stresses", London, UK, 1st December 1980, Digest No. 1980/72, pp. 2.1 - 2.5
- [14] Fort E. M., Pietsch H. E., "Aging of insulation by thermal and electrical stresses", Proceedings of the EIC 12th Electrical/Electronics Insulation Conference, Boston, MA, USA, 11-14 November 1975, IEEE Publ. No. 75 CH1014-0-EF54, pp. 143 - 146
- [15] Simoni L., "A new approach to the voltage-endurance test on electrical insulation", IEEE Transactions on Electrical Insulation, Vol. 8, No. 3, 1973, pp. 76 - 86
- [16] Simoni L., "A general approach to the endurance of electrical insulation under temperature and voltage", IEEE Transactions on Electrical Insulation, Vol. 16, No. 4, 1981, pp. 277 - 289
- [17] Simoni L., "General equation of the decline in the electric strength for combined thermal and electrical stresses", IEEE Transactions on Electrical Insulation, Vol. 19, No. 1, 1984, pp. 45 - 52
- [18] Ramu T. S., "On the estimation of life of power apparatus insulation under combined electrical and thermal stress", IEEE Transactions on Electrical Insulation, Vol. 20, No. 1, 1985, pp. 70 - 78
- [19] Ramu T. S., "Insulation failure modelling - Aspects in stochastic nature of failure", Proceedings of "A Short Term Course on Analysis of Failure of Insulation Systems", Indian Institute of Technology Madras, Chennai, India, 1-7 April 1998, pp. 16 - 20
- [20] Fallou B., Burguiere C., Morel J. F., "First approach on multiple accelerated life testing on electrical insulation", Annual Report on Electrical Insulation and Dielectric Phenomena (CEIDP), 1979, pp. 621 - 628
- [21] Eyring H., "The activated complex in chemical reactions", Journal of Chemical Physics, Vol. 3, No. 2, 1935, pp. 107 - 115
- [22] Koenig D., "Erfassung von Teilentladungen in Hohlraeumen von Epoxydharz-platen zur Beurteilung des Alterungsverhaltens bei Wechselspannung", Ph.D. Thesis, Technische Hochschule Braunschweig, Fakultae fuer Maschinenwesen, Braunschweig, Germany, 1967
- [23] Brunig A. M., Campbell F. J., Kasture D. G., Turner N. H., "Voltage induced insulation aging - Chemical deterioration from sub-corona currents in polymer void occlusions", Research Project Number: RP8007-1, July 1990, Naval Research Laboratory, Washington, D.C., USA, Project Manager: T. J. Rodebaugh
- [24] Brunig A. M., Campbell F. J., Kasture D. G., Turner N. H., "Effect of cavity sub-corona current on polymer insulation life", IEEE Transactions on Electrical Insulation, Vol. 26, No. 4, 1991, pp. 826 - 836
- [25] Tanaka T., Okamoto T., Nakanishi K., Miyamoto T., "Aging and related phenomena in modern electric power systems", IEEE Transactions on Electrical Insulation, Vol. 28, No. 5, 1993, pp. 826 - 844
- [26] Densley J., Bartnikas R., Bernstein B. S., "Multi-stress ageing of extruded insulation systems for transmission cables", IEEE Electrical Insulation Magazine, Vol. 9, No. 1, 1993, pp. 15 - 17
- [27] Brunig A. M., Danikas M. G., "Observations on discharges above and below CIV in polymer insulation", 1991 Annual Report on Conference on Electrical Insulation and Dielectric Phenomena, Knoxville, Tennessee, USA, 20-23 October 1991, pp. 638 - 647
- [28] Danikas M. G., Sarathi R., "Very small partial discharges and charging phenomena below inception voltage: An effort for a review and a proposal for a unified theory", FunkTechnikPlus#Journal, Issue 33, Year 11, 2024, pp. 7 - 27  
["https://www.ftpj.otoiser.org/issues/html/ftpj-issue-33-lo7532-export-ia1.htm"](https://www.ftpj.otoiser.org/issues/html/ftpj-issue-33-lo7532-export-ia1.htm) (33-1)

- [29] Danikas M. G., Sarathi R., "Some thoughts on charging phenomena in high-voltage insulating materials", *Journal of Engineering Science and Technology Review*, Vol. 14, No. 7, 2022, pp. 63 - 66 (special issue in honour of Prof. T. Tanaka)
- [30] Danikas M. G., Sarathi R., "Partial discharges in solid insulation cavities: Basic concepts, definitions and some thoughts for further research", *FunkTechnikPlus# Journal*, Issue 35, Year 12, 2024, pp. 5 - 24  
["https://www.ftpj.otoiser.org/issues/html/ftpj-issue-35-lo7532-export-ia1.htm"](https://www.ftpj.otoiser.org/issues/html/ftpj-issue-35-lo7532-export-ia1.htm) (35-1)
- [31] Vardakis G. E., Danikas M. G., Achillides Z., "A short review on charge packets and space charge properties inside dielectrics", *Engineering, Technology & Applied Science Research*, Vol. 13, No. 6, 2023, pp. 12211 - 12219
- [32] Haque S. M., Rey J. A. A., Umar Y., "Electrical properties of different polymeric materials and their applications: The influence of electric field," in *Polymer Dielectrics: Properties and Applications of Polymer Dielectrics*, Rijeka, Croatia: IntechOpen, 2017, pp. 41 - 63
- [33] Montanari G. C., Seri P., and Dissado L. A., "Discovery of an unknown conduction mechanism in insulating polymers", *High Voltage*, vol. 5, No. 4, 2020, pp. 403 - 408, "<https://doi.org/10.1049/hve.2019.0355>"
- [34] Kelen A., "Studies on partial discharges on solid dielectrics: A contribution to the discharge resistance testing of insulating materials", *Acta Polytechnica Scandinavica, Electrical Engineering Series*, EI-16, 1967, total number of pages 138, Stockholm, Sweden
- [35] Bartnikas R., "Commentary on partial discharge measurement and detection", *IEEE Transactions on Electrical Insulation*, Vol. 22, No. 5, 1987, pp. 629 - 653
- [36] Krause G., "Leitungsmechanismen und Raumladungsphänomene in Polyolefinen bei Hochfeldbeanspruchung", Ph.D. Thesis, RWTH Aachen, Germany, 1991
- [37] Holboll J. T., "The resistance of composite materials against electrical discharges - Partial discharges in voids in epoxy plastic", Ph. D. Thesis, Technical University of Denmark, Lyngby, Denmark, 1992
- [38] Bartnikas R., Novak J. P., "On the spark to pseudoglow and glow discharge Mechanism and discharge detectability" *IEEE Transactions on Electrical Insulation*, Vol. 27, 1992, pp. 3 - 14
- [39] Naidu S., Prabbashanker V., "Measurements of partial discharges - Corrections to erroneous counts occurring in a cumulative pulse-counting system", *Journal of Physics E: Scientific Instruments*, Vol. 10, 1977, pp. 1129 - 1132
- [40] Gulski E., "Computer-aided recognition of partial discharges using statistical tools", Ph.D. Thesis, Technical University of Delft, The Netherlands, 1991
- [41] Krivda A., "Recognition of discharges - Discrimination and classification", Ph.D. Thesis, Technical University of Delft, The Netherlands, 1995
- [42] Sletbak J., "Partial discharge measurements - Possibilities and limitations", *Proceedings of the 4th International Conference on Conduction and Breakdown in Solid Dielectrics*, Sestri Levante, Italy, 22-25 June, 1992, pp. 145 - 149
- [43] Danikas M. G., "Some possible new applications of a partial-discharge (PD) Model and its relation to PD-detection sensitivity", *European Transactions on Electrical Power (ETEP)*, Vol. 6, No. 6, 1996, pp. 445 - 448
- [44] Brancato E. L., "Status of aging in insulation materials and systems", *Proceedings of the 1st International Conference on Properties and Applications of Dielectric Materials*, Xi'an, China, 24-29 June 1985, Paper I-7
- [45] Turner N. H., Campbell F. J., Bruning A. M., Kasture D. G., "Surface changes of polymer cavities with currents above and below corona inception voltage", 1992 Annual Report on Conference on Electrical Insulation and Dielectric Phenomena, Victoria, B.C., Canada, 18-21 October 1992, pp. 687 - 693
- [46] Bruning A. M., Danikas M. G., "Experiments on polymer cavity currents above and below CIV", 1992 Annual Report on Conference on Electrical Insulation and Dielectric Phenomena, Victoria, B.C., Canada, 18-21 October 1992, pp. 735 - 740

- [47] Brancato E. L., Johnson L. M., Campbell F. J., Walker H. P., "Reliability prediction studies on electrical insulation: navy summary report", Naval Research Laboratory, Washington, D.C., NRL report 8095, 1977
- [48] Bartnikas R., "Some observations on the character of corona discharges in short gap spaces", IEEE Transactions on Electrical Insulation, Vol. 6, No. 2, 1971, pp. 63 - 75
- [49] Bartnikas R., "Corona discharge processes in voids", Engineering Dielectrics, Vol. I, Corona Measurement and Interpretation, ASTM Special Technical Publication 669, 1979, pp. 22 - 67
- [50] Bartnikas R., "Corona pulse counting and pulse-height analysis techniques", Engineering Dielectrics, Vol. I, Corona Measurement and Interpretation, ASTM Special Technical Publication 669, 1979, pp. 285 - 326
- [51] Kelen A., "Reflections on the long-term performance of electrical insulation", Revue Generale d' Electricite, Vol. 8, 1990, pp. 8 - 13
- [52] Kelen A., Danikas M. G., "Evidence and presumption in PD diagnostics", IEEE Transactions on Dielectrics and Electrical Insulation, Vol. 2, No. 5, 1995, pp. 780 - 795
- [53] Kelen A., "Critical examination of the dissipation factor tip-up as a measure of partial discharge intensity", IEEE Transactions on Electrical Insulation, Vol. 13, 1978, pp. 14 - 24
- [54] Kelen A., "Trends in PD diagnostics: When new options proliferate, so do problems - old and new", IEEE Transactions on Dielectrics and Electrical Insulation, Vol. 2, 1995, pp. 529 - 534
- [55] Dorris D. L., Pace M. O., Blalock T. V., Alexeff I., "Current pulses during water treeing detection system", IEEE Transactions on Dielectrics and Electrical Insulation, Vol. 3, No. 4, 1996, pp. 515 - 522
- [56] Dorris D. L., Pace M. O., Blalock T. V., Alexeff I., "Current pulses during water treeing procedures and results", IEEE Transactions on Dielectrics and Electrical Insulation, Vol. 3, No. 4, 1996, pp. 523 - 528
- [57] Morel O., Srinivas N., Bernstein B., "Partial discharge signals from TR-XLPE Insulated cable", Conference Record of the 2004 IEEE International Symposium on Electrical Insulation Indianapolis, IN, USA, 19-22 September 2004, pp. 466 - 470
- [58] Proceedings: Water Treeing and Aging, 1990 EPRI Workshop, EL-7479 Research Project 2957-78, October 1991, Phoenix, Arizona, December 9-11, 1990, Principal Author/Editor: A. T. Bulinski
- [59] Tanaka T., "Space charge injected via interfaces and tree initiation in polymers", IEEE Transactions on Dielectrics and Electrical insulation, Vol. 8, No. 5, 2001, pp. 733 - 743
- [60] Baumann T., Fruth B., Stucki F., Zeller H. R., "Field-enhancing defects in polymeric insulators causing dielectric aging", IEEE Transactions on Electrical Insulation, Vol. 24, No. 6, 1989, pp. 1071 - 1076
- [61] Zeller H. R., "Prebreakdown in diverging fields", 1990 Annual Report of C Conference on Electrical Insulation and Dielectric Phenomena (CEIDP), Pocono Manor, Pennsylvania, USA, 28-31 October 1990, pp. 457 - 464
- [62] Bell W. R., "Influence of specimen size on the dielectric strength of electrical insulation", Ph.D. Thesis, University of Newcastle-upon-Tyne, UK, 1974

# The Subtle Details of Combining the Arts of Antenna Design, Construction, and Measurement - The Radial Discone Paradigm -

N. I. Yannopoulou and P. E. Zimourtopoulos

Antennas Research Group, Austria - [www.op4.eu](http://www.op4.eu)

## Abstract

In the past, after the encouraged results produced by the first author and published in her master thesis regarding in essence the discone antenna, we decided to cooperate for the complement and extension of her work in the definite way of completely revealing all the subtle details of the whole work we are doing in general, in order to successfully combine the separate arts of antenna design, antenna construction, and antenna measurement, taking this particular antenna just as a concrete paradigm of practical application. Now, we describe in this paper the aforementioned way of ours and present the good agreement between the related analytical, computational, and experimental results, that we achieved working in this very way.

## Keywords

Broadband antennas, antennas analysis, antenna simulation, antenna construction, antenna measurements

## Introduction

A short history directly related with our research for the well-known broadband discone antenna includes its invention by Kandoian in 1945 [1], Nail's relations for its design in 1953 [2], Rappaport's design with N-type male connector feed in 1987 [3], Cooke's wire radial implementation in 1993 [4], and our previous work as it is presented in [5] and [6].

A typical 2D representation of the discone antenna is shown in Fig. 1 with its geometric characteristics:  $D$  is the disk diameter ( $t$  is its radius),  $d$  is the small (upper) diameter of the frustum cone,  $C$  is the large (lower) diameter of the frustum cone,  $s$  is the slant height, " $a$ " is the flare-angle and  $g$  is the spacing (gap) between disk and cone. Nails's relations are:

$$s = u (\lambda_1/4), D = v C, g = w d \quad (1)$$

where  $\lambda_1$  is the wavelength at the lowest "operating frequency"  $f_1$ , and the parameters are:

$$u = 1, v = 0.7, w = 0.3 \quad (2)$$

Rappaport proposed slightly different parameters:

$$u = 1.15, v = 0.75, w = 0.5 \quad (3)$$

while Cooke gave different  $u$  value:

$$u \approx 1.33 \quad (4)$$

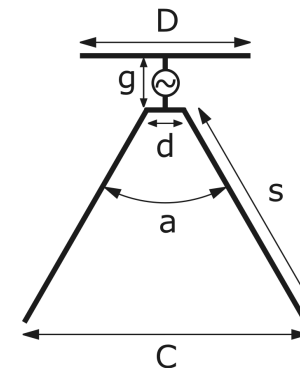


Fig. 1: Discone antenna

Full results of the twenty constructed and measured models of the radial discone antenna, i.e. a radial outline of discone, as well as some details for their fixed construction and the performed analytical study is presented

as an extended report. A description of the developed software for the radial discone antenna is given. The two first models were used in order to test our geometric representation of the antenna and the adopted simulation model which was finalized by the actual measurements.

After that, the rest eighteen experimental models with flare-angles  $a = 60^\circ$ ,  $a = 90^\circ$  and  $a = 120^\circ$  were carefully built according to the results and conclusion of the extended simulation investigation presented in [6] based on the definition we gave for the "Overall Antenna Bandwidth" in the same work, applied for three quantities of different nature with the following demands:

- a)  $Q_{SWR}: SWR \leq 2$
- b)  $Q_{Gp}: -3dB \leq G_{pH} \quad (5)$
- c)  $Q_{\mathcal{U}}: -3dB \leq \mathcal{U}_H$

with SWR as the circuit quantity, the horizontal directivity/power gain  $G_{dH}/G_{pH}$  as the field quantity and the horizontal radiation intensity  $\mathcal{U}_H$  as the field - circuit quantity. Their impedances and radiation patterns were measured up to the available VNA limit of 1300 MHz, confirming the omnidirectional radiation pattern.

The antennas were constructed with bare copper wire and fed by an N-type female connector. The simulation was based on a suite of developed visual tools supported by a fully analyzed, corrected and redeveloped edition of the original thin-wire computer program by Richmond [7]. The measurements were carried out with our measurement system in the anechoic chamber and the uncertainties in SWR, antenna impedance and radiation pattern were determined using the two methods fully described in [8] and [9]. Measurement uncertainties were estimated by DER clusters and their DEI stripes. Good agreement was observed between analytic, experimental and computational results.

### Radial discone study

The radial discone was analytically studied considering Standing Waves SW, that is, with symmetric sinusoidal current distribution:

$$\dot{I}(\ell) = \dot{I} \sin(\beta(h - |\ell|)), \quad (6)$$

$$-h \leq \ell \leq +h$$

and this current (6) was used to determine the antenna pattern by the formulas [10]:

$$\vec{E} = \left(\frac{1}{\lambda}\right) e^{i\beta R_{kr}} \text{PF} \begin{bmatrix} \ell_\theta \\ \ell_\phi \end{bmatrix} \quad (7)$$

$$\text{PF} = \int_{\ell_A}^{\ell_T} \dot{I}(\ell) e^{i\beta \ell_r \ell} d\ell \quad (8)$$

with the evaluation of the definite integral for Pattern Factor PF [11], [12]. The radial counterpart of the discone that was selected to be studied was the one with eight 8 radials for both the disk and the cone, as the most common in use. The coordinate system of Fig. 2 was adopted, where the disk is on xOy plane with its first radial on Ox and the cone is below xOy plane with its axis on the -z axis and with its radials exactly below the corresponding disk radials. Since the antenna has a geometric cylindrical symmetry is expected that it will have a uniform pattern on the horizontal plane. An antenna section is shown in Fig. 3 with the feed point source in magnification and the considered directions of currents while Fig. 4 shows in (a) and (b) the currents on the disk and cone radials respectively and in (c) their unit direction vectors  $\vec{e}_i$ . It is proved by implementation of the method of moments technique, that the currents are all equal to each other on the disk radials, that is equal to  $(1/8)\dot{I}$ , and all equal to each other on the cone radials, that is equal to  $(1/8)\dot{I}$ .

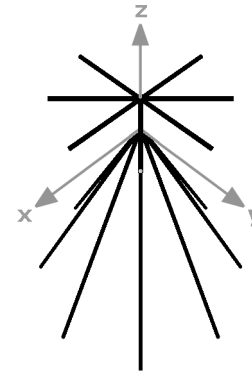


Fig. 2: Disk-Cone 3D Model

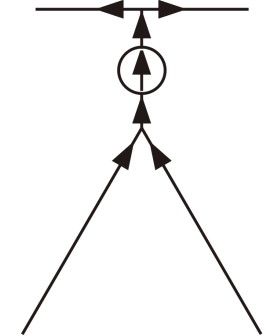


Fig. 3: Radial currents

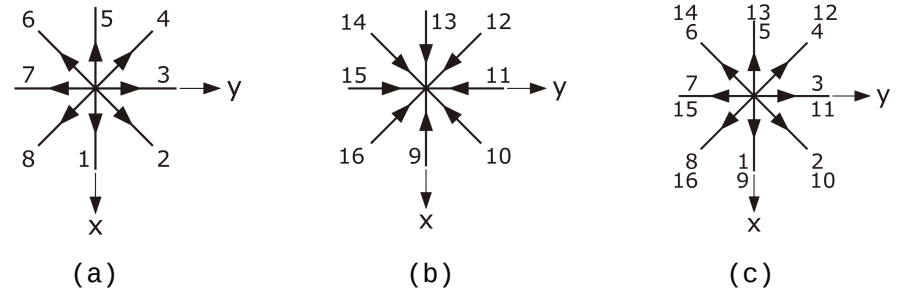


Fig. 4: Currents and unit direction vectors

It is also proved that the radials of the disk, as well as the radials of the cone, form a uniform circular array UCA [10], [12] of monopoles. If we consider the first radial, that on Ox for the disk, as the generator of the disk array and the current ratio as

$$I_v = \frac{\dot{I}_v}{\dot{I}_1} \quad (9)$$

then the electrical condition of an UCA which is given by

$$|I_v| = 1 = \frac{|\dot{I}_v|}{|\dot{I}_1|}, \quad e^{i\dot{I}_v} = e^{i(v-1)\gamma} \quad (10)$$

where

$$\angle \dot{I}_{k+1} - \angle \dot{I}_k = \gamma \Rightarrow \gamma_v = (v-1)\gamma \quad (11)$$

and the geometrical condition which demands two successive antennas to arise from each other by rotation of the one

by a fixed angle, that is:

$$\alpha_v = \frac{2\pi(v-1)}{N}, \quad 0 \leq \alpha_v < 2\pi \quad (12)$$

where  $\alpha_v$  is the oriented angle between the first and the  $v$ -th element of the array and  $N$  stands for the total number of elements, are both satisfied. The same is true for the radials of the cone with the corresponding quantities in (9) - (12) with a prime symbol.

Furthermore, it is obvious that the elements of both the UCA arrays have the same initial point, the origin of the selected coordinate system, where the source is located, that is, the same position vector  $\vec{R}_v = \vec{R}'_v = \vec{0}$ , but with opposite currents  $\vec{I}_v = -\vec{I}'_v$  and as it has been already mentioned the same corresponding angle,  $\alpha_v = \alpha'_v$ . Thus, we may consider one array consisting of doublets of monopoles in a V arrangement.

After manipulation of the rather lengthy relations for the radiation pattern of such an array of  $N$  V-dipoles and by defining the following quantities

$$\xi \equiv 180^\circ - \frac{a}{2} \quad (13)$$

$$k \equiv \frac{\sin(\beta t)}{\sin(\beta s)} \quad (14)$$

$$\dot{I} = \frac{\dot{I}_{inp}}{2\pi N \sin(\beta t)} \quad (15)$$

$$\varphi'_v = \varphi - \alpha_v \quad (16)$$

$$p \equiv \sin\theta \cos\varphi'_v \quad (17)$$

$$q \equiv p \sin\xi + \cos\xi \cos\theta \quad (18)$$

$$\dot{F}_v \equiv \frac{e^{i\beta xy} - (\cos(\beta x) + i y \sin(\beta x))}{1 - y^2} \quad (19)$$

$$\dot{A}_v = \dot{F}_v(\delta, p) \quad (20)$$

$$\dot{B}_v = \dot{F}_v(s, q) \quad (21)$$

the antenna pattern is

$$\vec{E} = \begin{bmatrix} \dot{E}_\theta \\ \dot{E}_\varphi \end{bmatrix} = \dot{I} \begin{bmatrix} \cos\theta \sum_{v=1}^N (\dot{A}_v - k \sin\xi \dot{B}_v) \cos\varphi'_v - \sin\theta k \cos\xi \sum_{v=1}^N \dot{B}_v \\ - \sum_{v=1}^N (\dot{A}_v - k \sin\xi \dot{B}_v) \sin\varphi'_v \end{bmatrix} \quad (22)$$

If the number  $N$  is even, as it is in the presented case of  $N = 8$  V-dipoles then (20) is simplified as

$$\dot{A}_v = i \frac{\sin(\beta\delta p) - p \sin(\beta\delta)}{1 - p^2} \quad (23)$$

### Radial Discone Antenna GUI Application

A visual program was specifically developed to design a broadband radial discone antenna with the initial window together with the available sub-menus and About shown in Fig. 5. This is mainly a general program to produce the geometry of a discone with bare wires embedded in free space when the wire conductivity, the type of feeding connector and the frequency band are given, as shown in Fig. 6. At the first frame on the top the number of disk and cone radials are given together with the number of segments per radial. At the second frame three choices are available for the antenna's dimensions according (1) - (3) under the option buttons [Kandoian-Nail], [Rappaport] and [Other] where we have to type the dimensions in [cm] and press ENTER in each text box in order to be saved. The flare angle is given in degrees [ $^\circ$ ], and the wire radius in [cm]. As feeding connector the types of N-male, N-female, SMA-male and SMA-female are available or [Other] where the diameter of the connector must be typed in [cm]. Two models can be created, the simple Disk-Cone model (Fig. 2) and the Disk-Frustum Cone model (Fig. 1) for simulation via [RICHWIRE].

Selecting [Frequency Sweep] check button the initial FA and final FB frequencies must be given with the desired step for an automatic simulation. The program saves all data, input and output, at a separate directory named from each frequency. The dialog box of Fig. 7 opens in order to select the Working Directory on the hard drive where these sub-directories will be created. The check boxes [Source] and [Show Geometry] create the antenna geometry file as 3D geo.wrl with a red spherical point to indicate the position of source. If the directory already exists then for data protection a different directory must be created as indicated in Fig. 8 and for a new directory the dialog box of Fig. 9 demands confirmation.

[RICHWIRE] runs at background and 4 files are generated: OUT.TXT with general information such as geometry, mutual impedance matrix, amplitude of dipole currents, OUT2D.TXT with radiation pattern in 3 main planes xOy, yOz, zOx, per  $1^\circ$ , OUT3D.TXT with radiation pattern in space per  $5^\circ$  and TOTAL.TXT file with the total number of segments, frequency, input impedance in Cartesian and polar form, VSWR for 50 Ohm and 75 Ohm, directivity as pure number and in dBi and dBd.

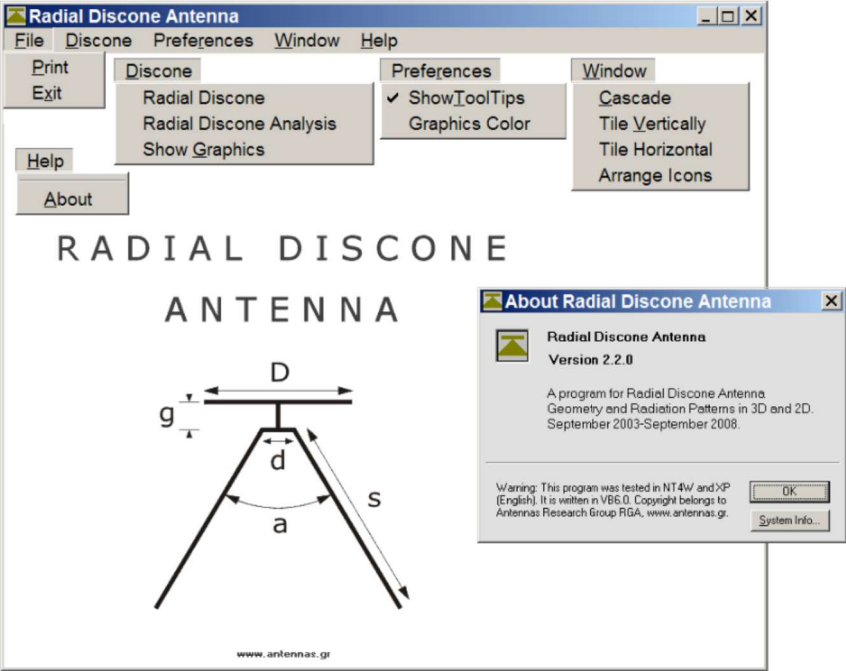


Fig. 5: Radial discone antenna GUI application

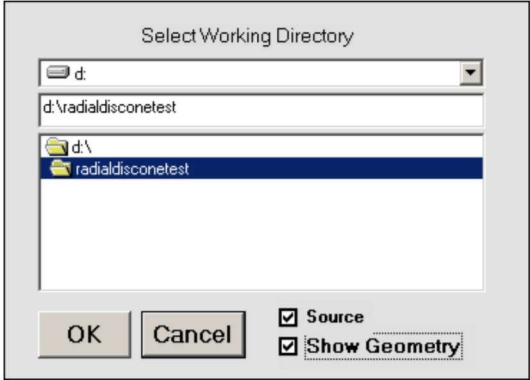


Fig. 7: Select Working Directory

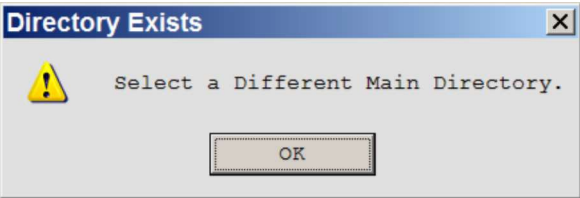


Fig. 8: Directory Exists

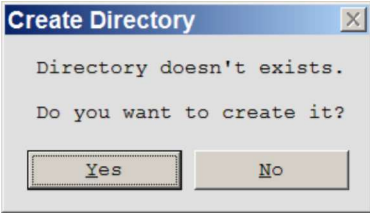


Fig. 9: Create Directory

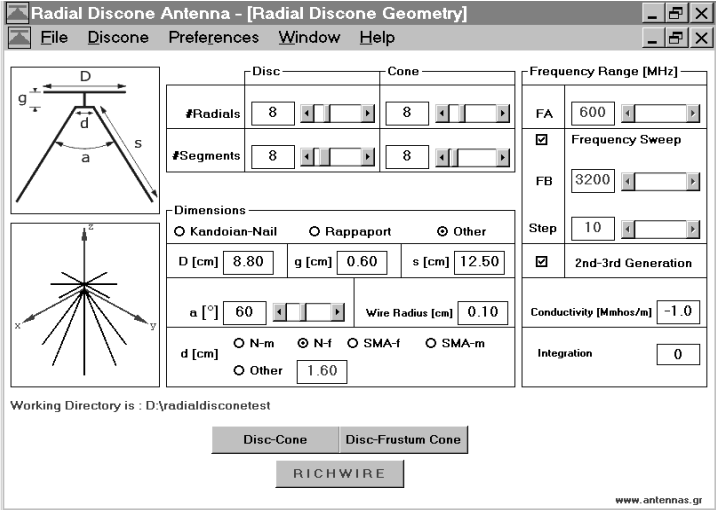
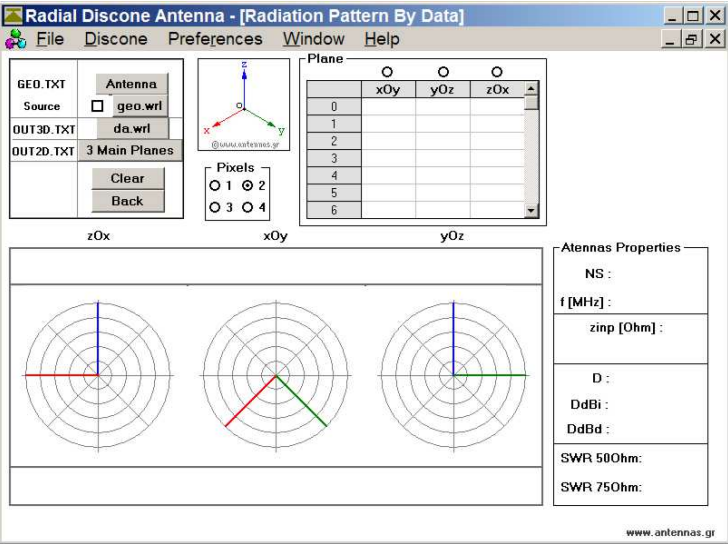
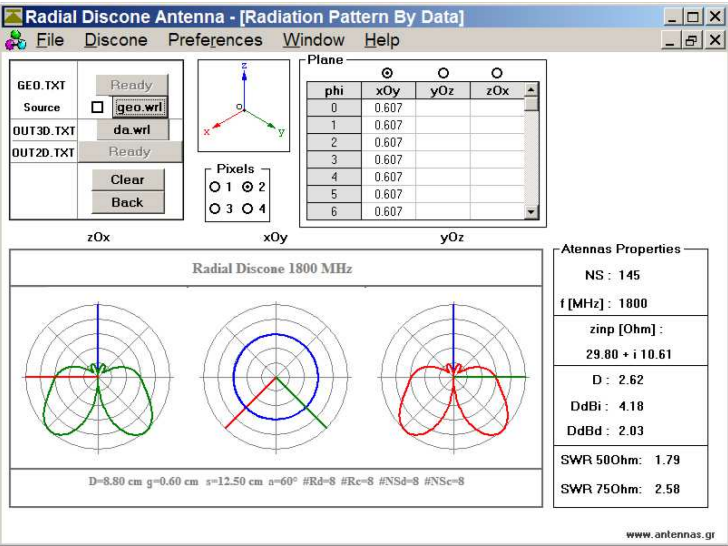


Fig. 6: Radial Discone Geometry

An additional TOTAL.TXT file will be created at the main directory with the above information for all frequencies in case of [Frequency Sweep]. The window [Show Graphics] of Fig. 10a is the same as described in detail by the authors in [13]. Fig. 10b shows as an example the results for one of the constructed antennas. The menu option [Radial Discone Analysis] opens the window [Radial Discone Geometry: Theory + Simulation] as shown in Fig. 11.



(a)



(b)

Fig. 10: Show Graphics window

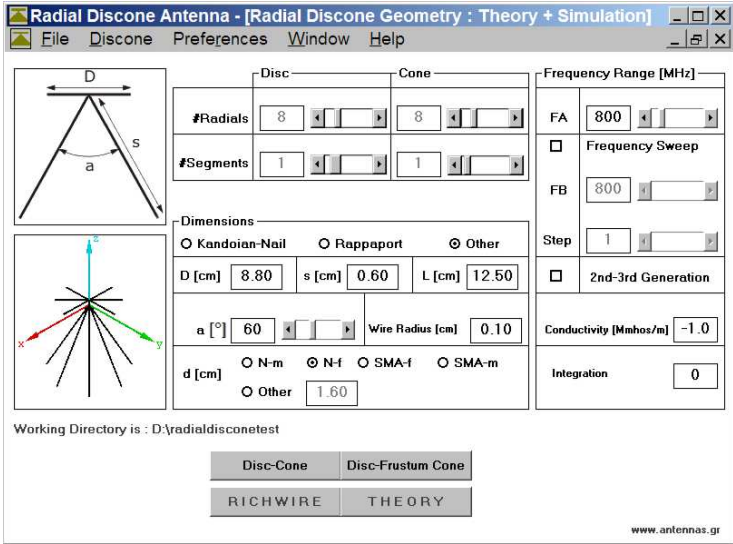


Fig. 11: Theory + Simulation window

Through this form an analytical evaluation of the antenna radiation pattern is possible from (22) where the number of radials and segments can not be changed. In fact only one (1) segment is considered per radial. This form although is still beta, provides in addition the possibility of simulation by either of the two models with 1 segment per radial for both disk and cone in order to obtain a more accurate comparison. It is evident that considering one segment per radial puts some limitation in term of frequency, as [RICHWIRE] demands the smaller segment to be about  $\lambda/4$ . To overcome this problem we removed the criteria that stop the

program execution. Other features of this application through its menu options are:

- a) [File-Print]: print the available windows,
- b) [Preferences-ShowToolTips]: enables or disables the short messages appearing when the mouse is over the various objects
- c) [Preferences-Graphics-Color]: change the colors of 2D-radiation patterns, and
- d) [Help-About]: gives general information as the important warning that the application was tested in NT4W and XP operating systems (English) as shown in Fig. 5.

### Construction details

It was deemed appropriate to provide some details about the construction of discone antennas to demonstrate the fact that what we learn in the first years of our education can be used and facilitate our practical applications. Thus, starting from the construction of a cone, truncated or not, we remember the paper constructions of solids. A key role for the cone flare angle,  $a$ , is played by the relationship

$$\omega = 360^\circ \frac{\text{cone base radius}}{\text{cone slant height}} \quad (24)$$

$$= 360^\circ \frac{C/2}{s} = 360^\circ \sin\left(\frac{a}{2}\right)$$

where relation (8) of [6]

$$C = 2s \sin(a/2) \quad (25)$$

has been used. Relation (24) gives the necessary circular sector in degrees that must be drawn to obtain a cone with a flare angle  $a$ . Then we divide the circular sector into as many radii as we want the discone antenna under construction to have.

Fig. 12 shows the corresponding circular sectors and their division into 8 radii for a cone with flare angle  $60^\circ$ ,  $90^\circ$  and  $120^\circ$ . The angle between two successive radii is also noted. The inner

small circle corresponds to the diameter of the connector. Fig. 13 shows the tools needed for their paper construction, and their corresponding photos. The margin at the end of the circular sectors was used to glue a circular base to the cones and thus making the paper construction more stable.

Three constructed frustum cones along with the wire models after soldering are shown in Fig. 14. In practice, the wire radial were held in place with tape and a wire ring of 1.6 cm diameter, the same as the diameter of the female N-type connector, was soldered to the small base of the truncated cones.

Fig. 15 shows how the radial disks were constructed. The male part of a type-N connector, pin, was fitted into a hole drilled in the center of a piece of wood and then the radials of the disk were kept in place to the wood with tape. After soldering, the pin was carefully pushed from underneath and we lifted the disk. Three such disks with different pin heights are shown in Fig. 16 while various parts of the constructions are shown in Fig. 17. The wire welding was carried out with tin and 100W soldering iron for the disk radials and 50W for the cone radials.

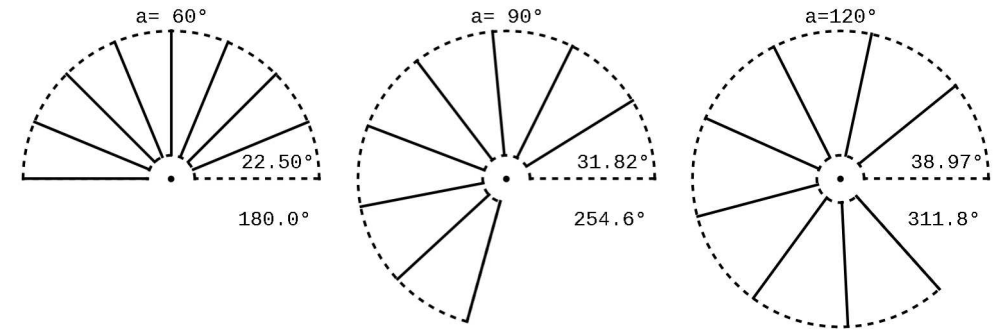


Fig. 12: Circular sectors for  $a = 60^\circ$ ,  $90^\circ$ ,  $120^\circ$

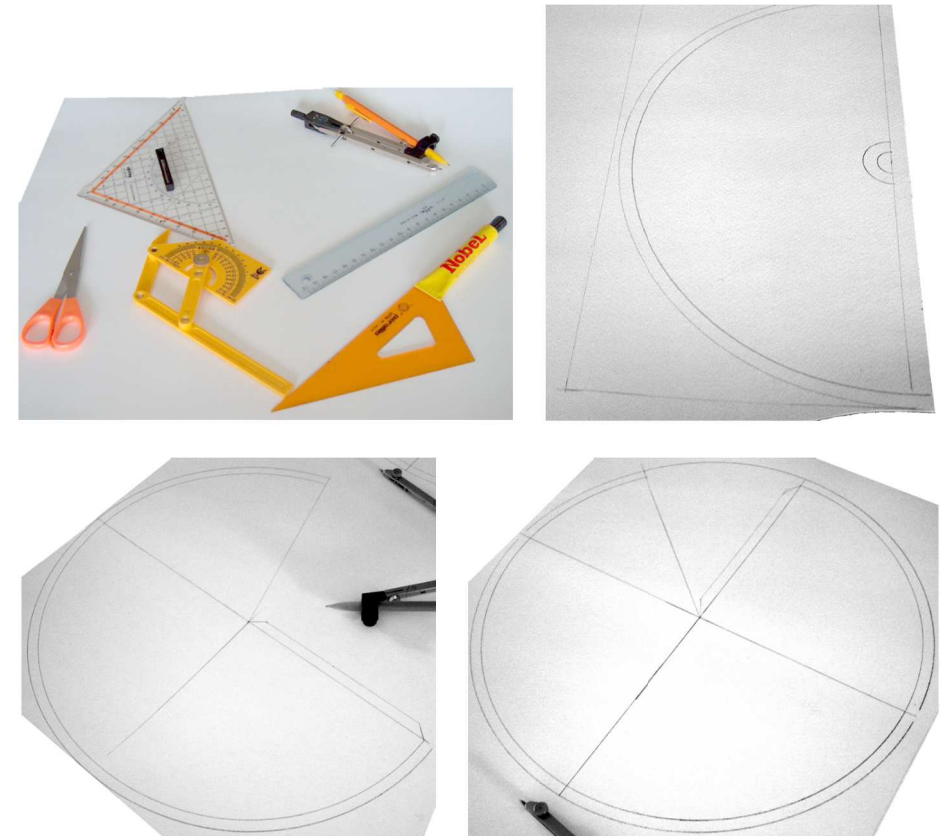


Fig. 13: Paper construction of cones

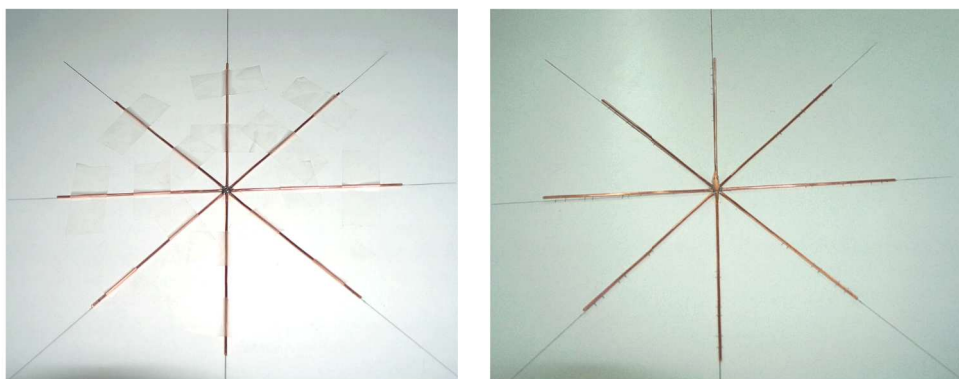
Fig. 14: Constructed frustum cones for  $\alpha = 60^\circ, 90^\circ, 120^\circ$ 

Fig. 15: Construction of disks

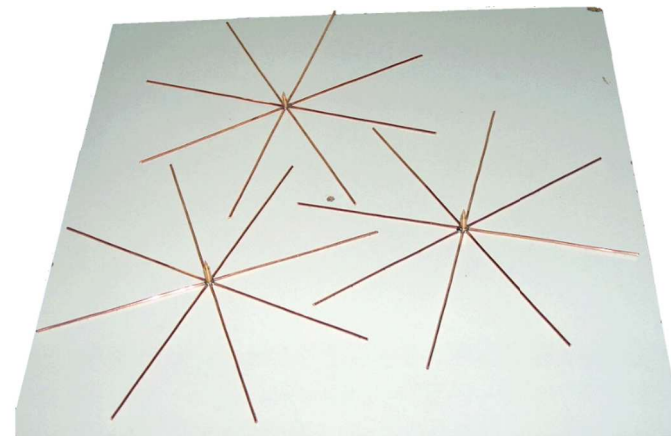
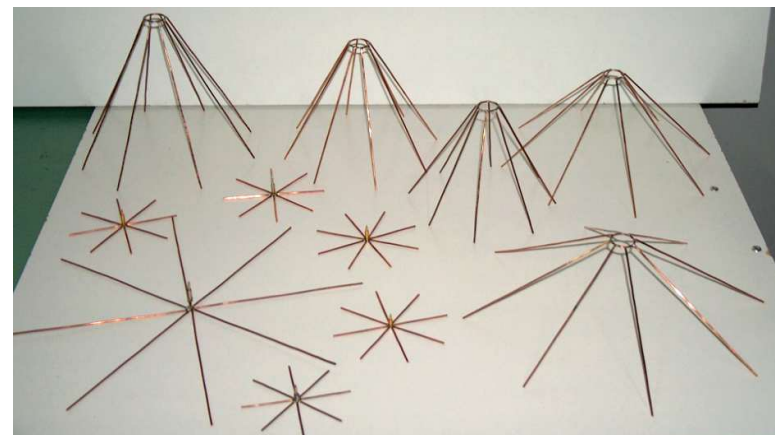
Fig. 16: Radial disks:  $g = 0.3 \text{ cm}, 0.6 \text{ cm}, 0.8 \text{ cm}$ 

Fig. 17: Parts of radial discons

**Test antennas**

The simplest simulation model for a radial discone antenna is the model Disk-Cone of Fig. 2. Two test antennas, shown in Fig. 18, were initially simulated, using this model, in the range of [400,

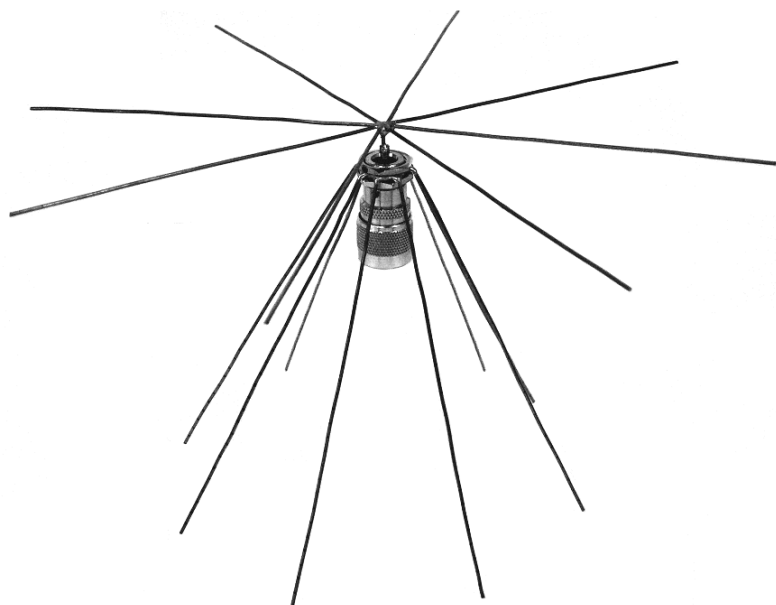
2500] MHz, constructed and measured in the range of [400, 1300] MHz. The first was a rather large discone antenna which did not follow any of the typical dimension standard, with slant height  $s = 15$  [cm], disk diameter  $D = 26$  [cm],

disk to cone space  $g = 1.5$  [cm] and cone flare-angle  $a = 60^\circ$ , shown in the anechoic chamber in Fig. 19. The second antenna was a rather small disccone antenna initially designed following the dimensions proposed by Nail (1)-(2) with  $s = 10.7$  [cm],  $D = 7.5$  [cm],  $g = 0.5$  [cm] and  $a = 60^\circ$ , in order to have  $\text{SWR} \leq 2$  at 800 [MHz]. The slant height was equal to  $\lambda/4$  at 700 [MHz], according to the relation of the cut off frequency  $f_c$ , where  $s$  is equal to  $\lambda/4$ , with respect to the lowest desired operational frequency  $f_1$  [14],

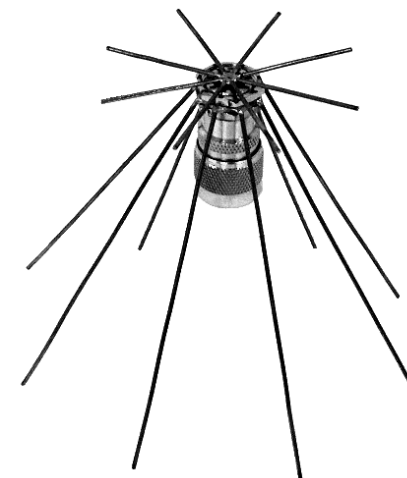
$$f_1 = 1.14 f_c \text{ for } a = 60^\circ$$

If  $f_1 = 800$  [MHz] then  $f_c = 800 / 1.14 = 701.8 \approx 700$  [MHz] and for a female Type N connector with diameter  $d = 1.6$  [cm],  $g = 0.3 \times 1.6 = 0.48 \approx 0.5$  [cm].

For both these test antennas an investigation was performed regarding the number of radials, the same for disk and cone, and the number of segments per radial to be used for simulation. Fig. 20 shows the results with respect to the power input in [dB]. Thus, 8 radials for both disk and cone and 8 segments per radial were selected for simulation.



(a)  $a = 60^\circ$ ,  $s = 15$  [cm],  $D = 26$  [cm],  $g = 1.5$  [cm]: T-L



(b)  $a = 60^\circ$ ,  $s = 10.7$  [cm],  $D = 7.5$  [cm],  $g = 0.5$  [cm]: T-S  
Fig. 18: Test disccone models - Large (T-L) and Small (T-S)

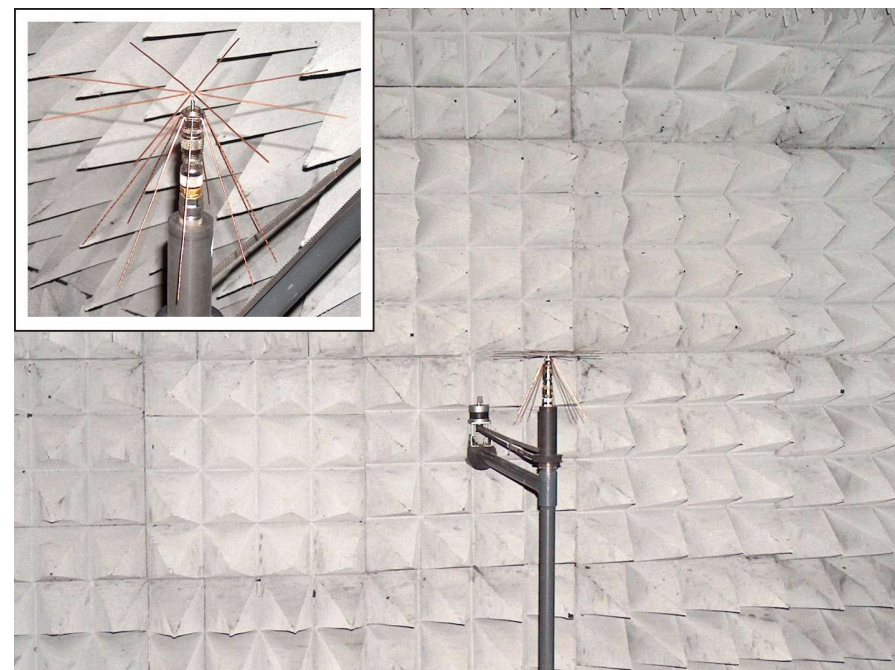


Fig. 19: Large test antenna in situ

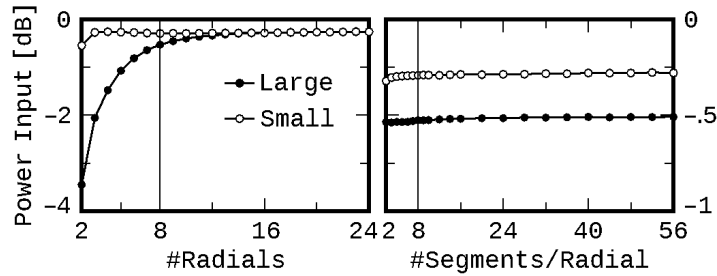


Fig. 20: Radials and segments

The divergence between measurements and simulation data for the antenna impedance showed that a more realistic simulation model had to be applied, that of the Disk-Frustum Cone of Fig. 21. The comparison between measurement results with their Differential Error Intervals (DEIs), as defined in [12], and simulation data, for both models, is shown in Fig. 22. The same figure also shows the curve of the processed measurements with a red line, as obtained by a sixth-degree polynomial fitting selected by inspection, that is, based on an optical argument, during the preparation of the master thesis [11]. This technique was applied to the impedance curves of the thesis, 20 for the real and 20 for the imaginary part, (Ch.5: pp. 8, 19, 35, 44, 53, 62, 71, 80, 90, 99, 108, 117, 126, 135, 145, 154, 163, 172, 181, 190) and for the corresponding SWR figures (pp. 6-4, 6-5, 6-10) and is not repeated here be-

cause they are too many. All the experimental results presented here are without any curve fitting.

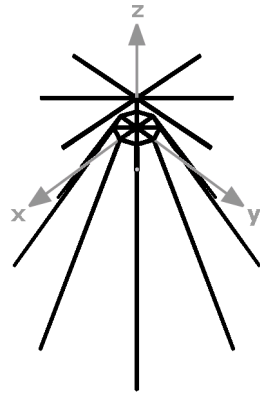


Fig. 21: Disk-Frustum Cone radial discone model

Tab. 1 shows the minimum, maximum and average deviation between the results from the processed measurements [11], and from the measurements, of both simulation models, Disk-Cone and Disk-Frustum Cone, for the real, the imaginary parts and the absolute value of the input impedance in ab-

solute and relative values with respect to the measurements. The symbols and relations used are:

$R^m$ ,  $X^m$ : Real and Imaginary parts of input impedance from measurements

$R^c$ ,  $X^c$ : Real and Imaginary parts of input impedance from simulation model Disk-Cone (c)

$R^f$ ,  $X^f$ : Real and Imaginary parts of input impedance from simulation model Disk-Frustum Cone (f)

$Z$ ,  $Z^c$ ,  $Z^f$ : Complex input impedance from measurements,

and simulation models c and f

$$\frac{1}{N} \cdot \sum_{v=1}^N |u_v^m - u_v^t|$$

mean deviation, where  $u^m$  corresponds to quantity from measurements and  $u^t$  to quantity from simulation

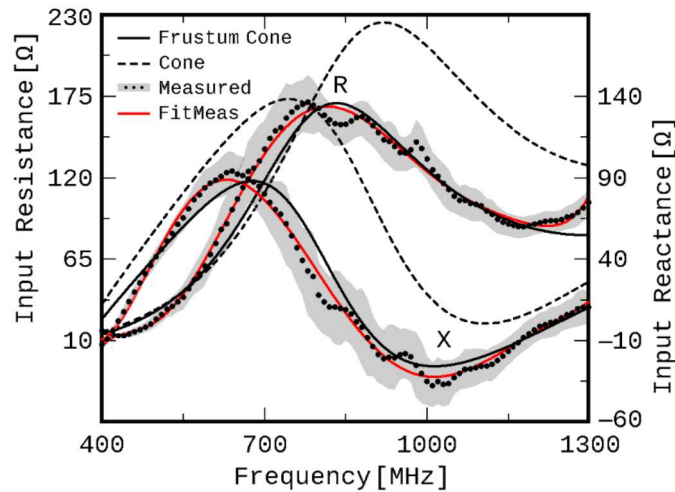
$$\frac{1}{N} \cdot \sum_{v=1}^N \frac{|u_v^m - u_v^t|}{|u_v^m|}$$

relative mean deviation as above

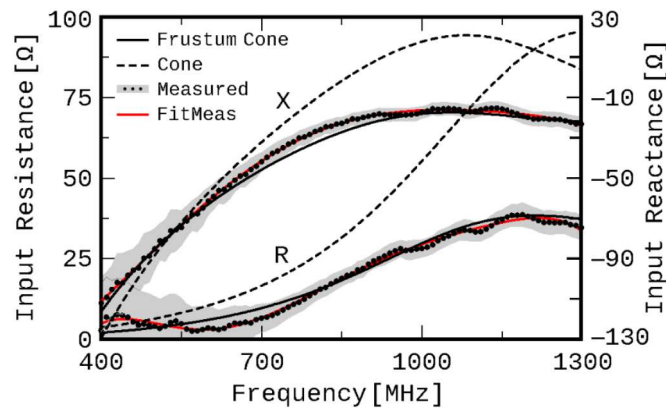
$\delta$ : Convergence index defined as the ratio of the mean deviations:  $f/c$ . Smaller values indicate a greater closeness between model f and measurements.

Tab. 1: Deviation of measurement and simulation results

		Min		Max		Mean		$\delta$	
		Fit	NoFit	Fit	NoFit	Fit	NoFit	Fit	NoFit
$ R^m - R^c $	[ $\Omega$ ]	0.1	0.3	61.7	60.9	21.5	21.6	0.07	0.08
$ R^m - R^f $	[ $\Omega$ ]	0.0	0.0	3.8	5.2	1.6	1.8		
$ X^m - X^c $	[ $\Omega$ ]	0.2	0.6	37.3	38.0	20.5	20.6	0.11	0.11
$ X^m - X^f $	[ $\Omega$ ]	0.0	0.0	5.1	6.1	2.3	2.3		
$ Z - Z^c $	[ $\Omega$ ]	2.7	2.2	67.8	66.7	30.6	30.6	0.10	0.10
$ Z - Z^f $	[ $\Omega$ ]	0.2	0.3	5.8	6.5	3.1	3.2		
$ Z - Z^c / Z $	[%]	3	3	164	160	80	80	0.09	0.10
$ Z - Z^f / Z $	[%]	0	0	16	20	7	8		



(a) Large radial discone antenna



(b) Small radial discone antenna

Fig. 22: Test antennas input impedance from simulation, measurement with curve fitting and measurement with DEIs

From this Tab. 1 it is obvious that the model of Disk-Frustum Cone is the most appropriate for our constructed antennas.

Simulation of the second antenna with the model of Disk-Frustum Cone proved that the condition of  $SWR \leq 2$  was satisfied for  $996 \leq f \leq 1496$  and  $2206 \leq f$  with a maximum value of 2.128 in the whole range 996-2500 [MHz]. Therefore, there was a significant difference from the initial design results with the Disk-Cone model, where  $SWR \leq 2$  was true for the range 800-2170 [MHz], as shown in Fig. 23. This fact led us to adopt Cooke's remark (4) for the radial discones which implies that the slant height must be equal to  $\lambda/3$  at the lowest desired frequency and for this specific antenna

$$\lambda = 3 \times 10.7 \times 10^{-2} = 0.321 \Rightarrow$$

$$\Rightarrow f_1 = \frac{300}{0.321} \approx 935 [\text{MHz}]$$

which proved to be nearly true from the measurements carried out. Finally, Fig. 24 shows the relative radiation intensity patterns for both Large and Small test discones at 800, 1000 and 1200 MHz.

### Simulation and Measurement

All the details for the simulation of the eighteen models that were selected to be constructed with cone flare angles  $60^\circ$  with the best performance,  $90^\circ$  as a marginal case and  $120^\circ$  the greater cone angle with satisfactory characteristics, by applying a mixture of directives by Cooke, Nail and Rappaport, were given in [6].

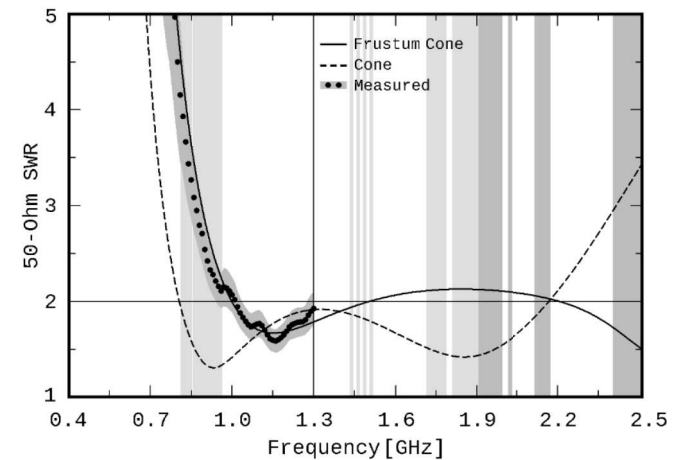


Fig. 23: SWR of small test discone antenna

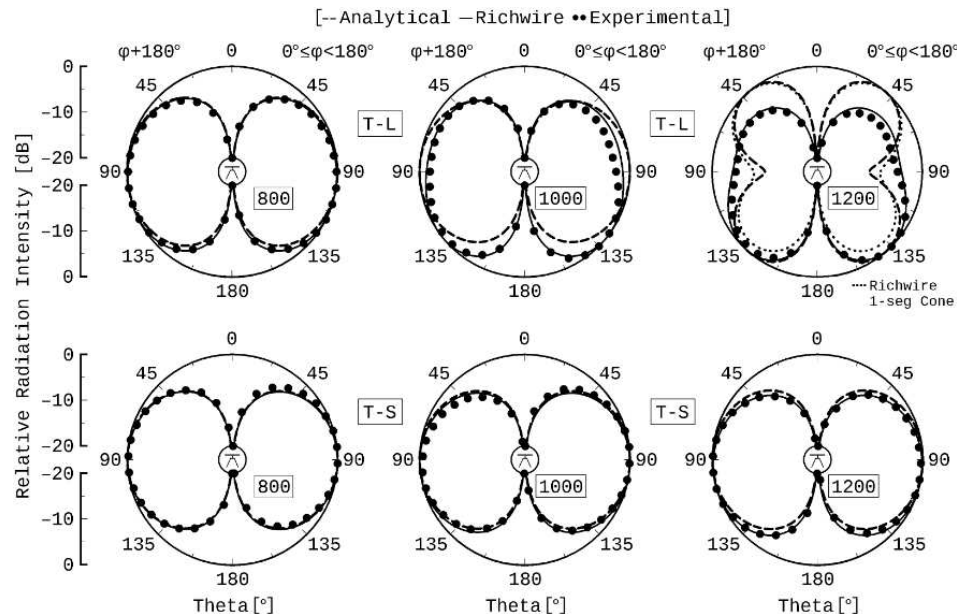


Fig. 24: Radiation intensity patterns for test antennas  
Analysis-Simulation-Measurement comparison

The antennas were divided into three groups A, B and C for each cone angle of 120°, 90° and 60° respectively as they are given in Tab. 2 according to their specific characteristics.

Fig. 25 shows three characteristic constructed antenna models for 60°, 90° and 120° flare angle. All the antennas have 8 radials for both cone and disk from copper wire, cone slant height 12.5 [cm] and constant small cone diameter equal to the N-type female connector diameter, 1.6 [cm].

The small differences be-

tween the six models of each group, A, B, C, did not present any significant difference in the radiation pattern. For this reason typical relative radiation patterns in a vertical plane with a comparison between analytical, simulation and experimental results are shown in Fig. 26 for 800, 900, 1000, 1100, 1200 and 1300 MHz where each column corresponds to 120°, 90° and 60° cone flare angle respectively. Figs. 27 - 32 shows input impedance as real R and imaginary X parts of the constructed antennas, as it was predicted by [RICH-

WIRE] and measured, with the choic chamber as described in detail in [8], [9] with the measurement system fully described in [11] and [12].

Tab. 2: Constructed antenna models

		g [mm]	0.3	0.6	0.8
A	a = 120°	D = 16.2 [cm]	A#1.1	A#1.2	A#1.3
		D = 15.2 [cm]	A#2.1	A#2.2	A#2.3
B	a = 90°	D = 13.2 [cm]	B#1.1	B#1.2	B#1.3
		D = 12.4 [cm]	B#2.1	B#2.2	B#2.3
C	a = 60°	D = 9.4 [cm]	C#1.1	C#1.2	C#1.3
		D = 8.8 [cm]	C#2.1	C#2.2	C#2.3

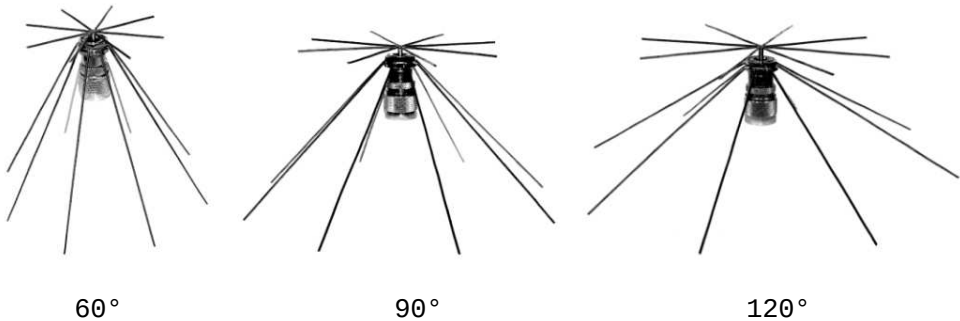


Fig. 25: Constructed antennas

While the agreement between the simulation and experimental results is very good, it is nevertheless clear that there is a ripple in the measurements for all antennas, in terms of impedance. We have taken special care to keep the same reference plane for all measurements, those

of standard loads and of the antennas, adopting the construction technique we described above, assuming that this will reduce if not eliminate the influence of the transmission line. In an attempt to explain this ripple or even predict it, we added to the simulation the inevitably existing transmission line as two cylindrical sections of 8 wires each with the lengths 23 cm and 102 cm and position in space exactly as shown in Fig. 19 inside the anechoic chamber. In Fig. 33 are given indicatively the results for three antennas: A#1.3, B#2.3 and C#2.2, where a similar ripple appears to be reproduced by simulation

data. However, further research is needed on this issue. Finally, Fig. 34 shows the SWR for three antennas: A#2.2, B#2.2 and C#2.2 with a maximum value of SWR=3 which corresponds to 25% reflected power. We observe that the shape of the curve is maintained and in fact the measurements almost all give a lower SWR compared to the corresponding calculations. This fact is a strong indication that the agreement between measurements and predictions is expected to be equally good for the rest of simulation frequency range for which we do not yet have the appropriate measuring instruments.

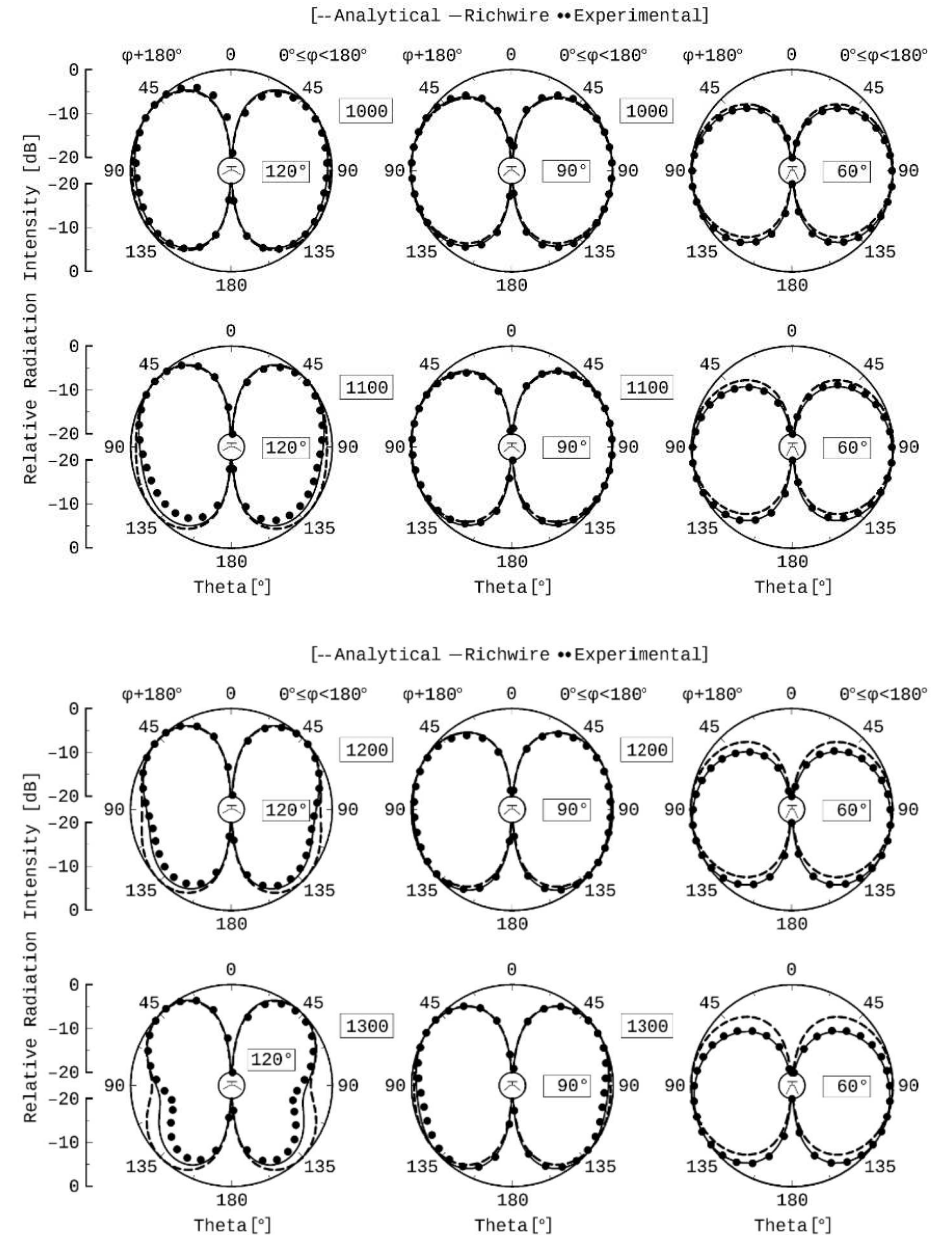
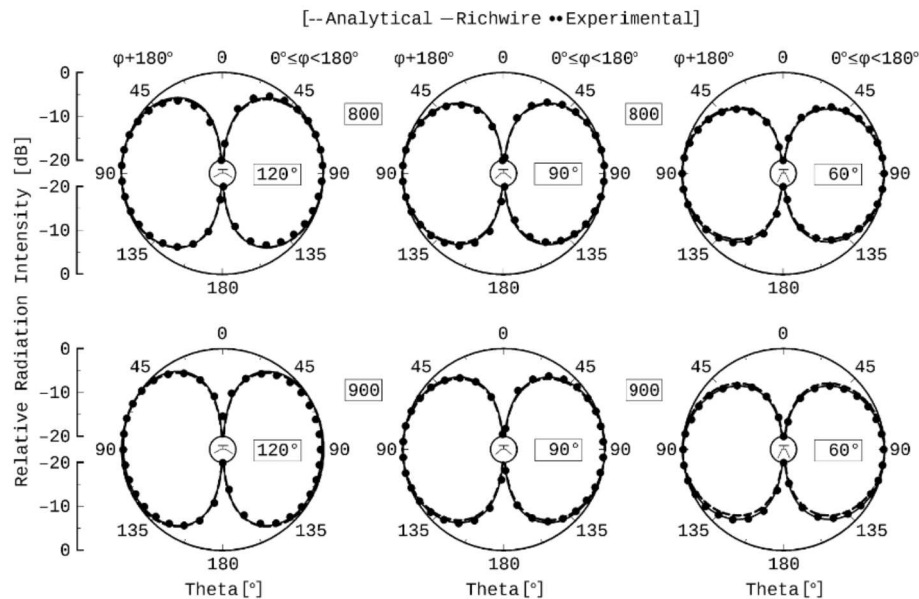


Fig. 26: Radiation intensity pattern on a vertical plane

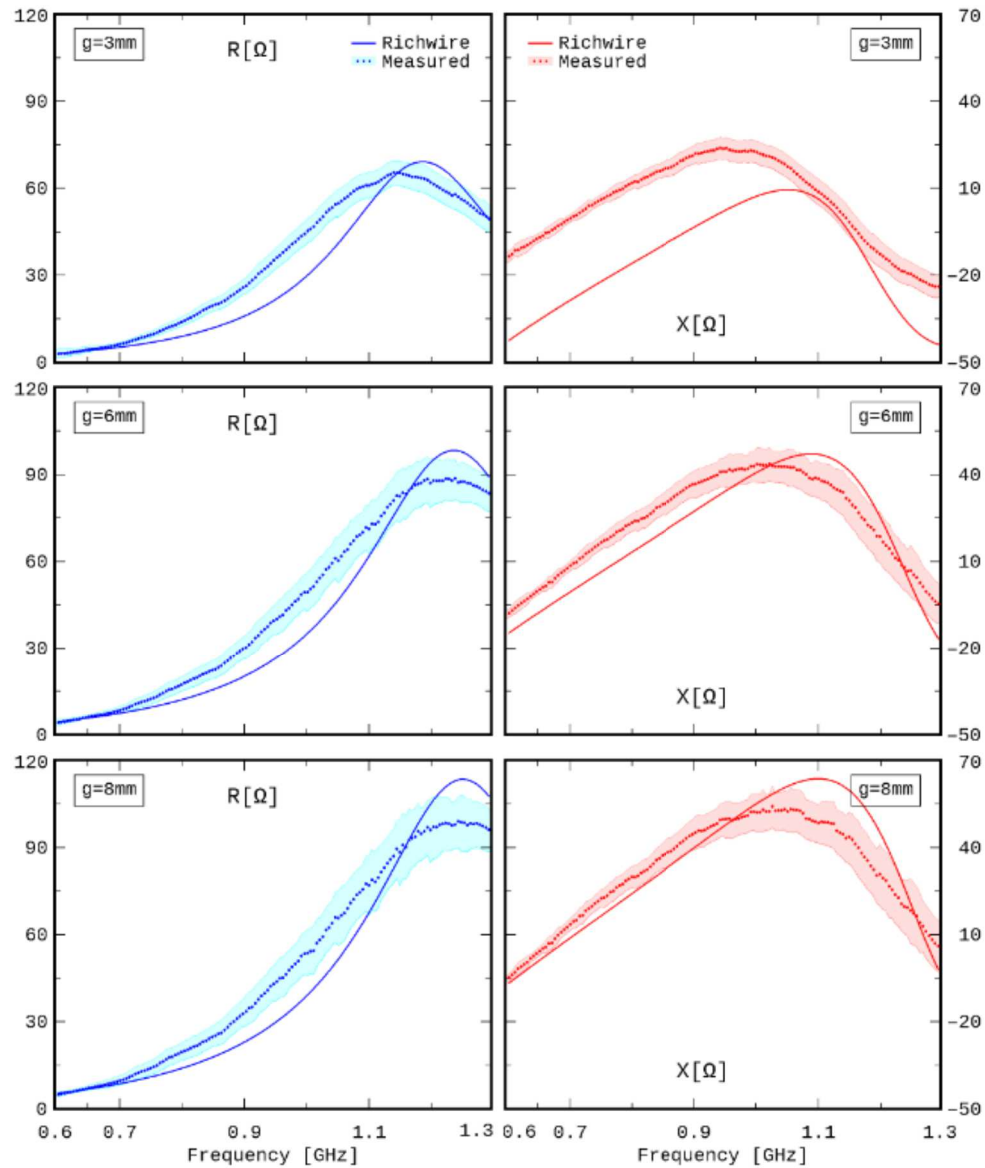
$a = 120^\circ$ ,  $D = 16.2$  cm,  $s = 12.5$  cm,  $d = 1.6$  cm


Fig. 27: Input impedance for A#1.1, A#1.2, A#1.3 models

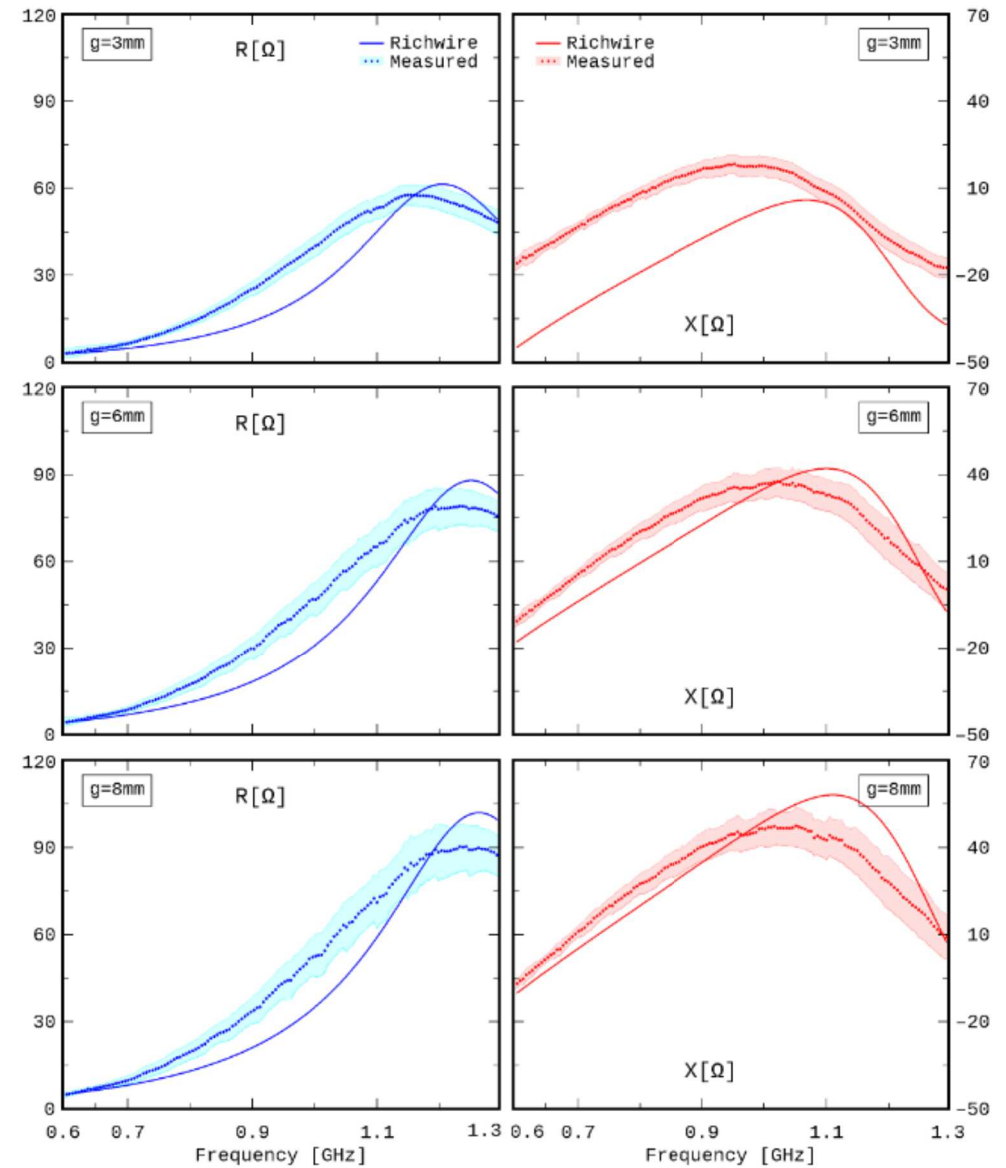
 $a = 120^\circ$ ,  $D = 15.2$  cm,  $s = 12.5$  cm,  $d = 1.6$  cm


Fig. 28: Input impedance for A#2.1, A#2.2, A#2.3 models

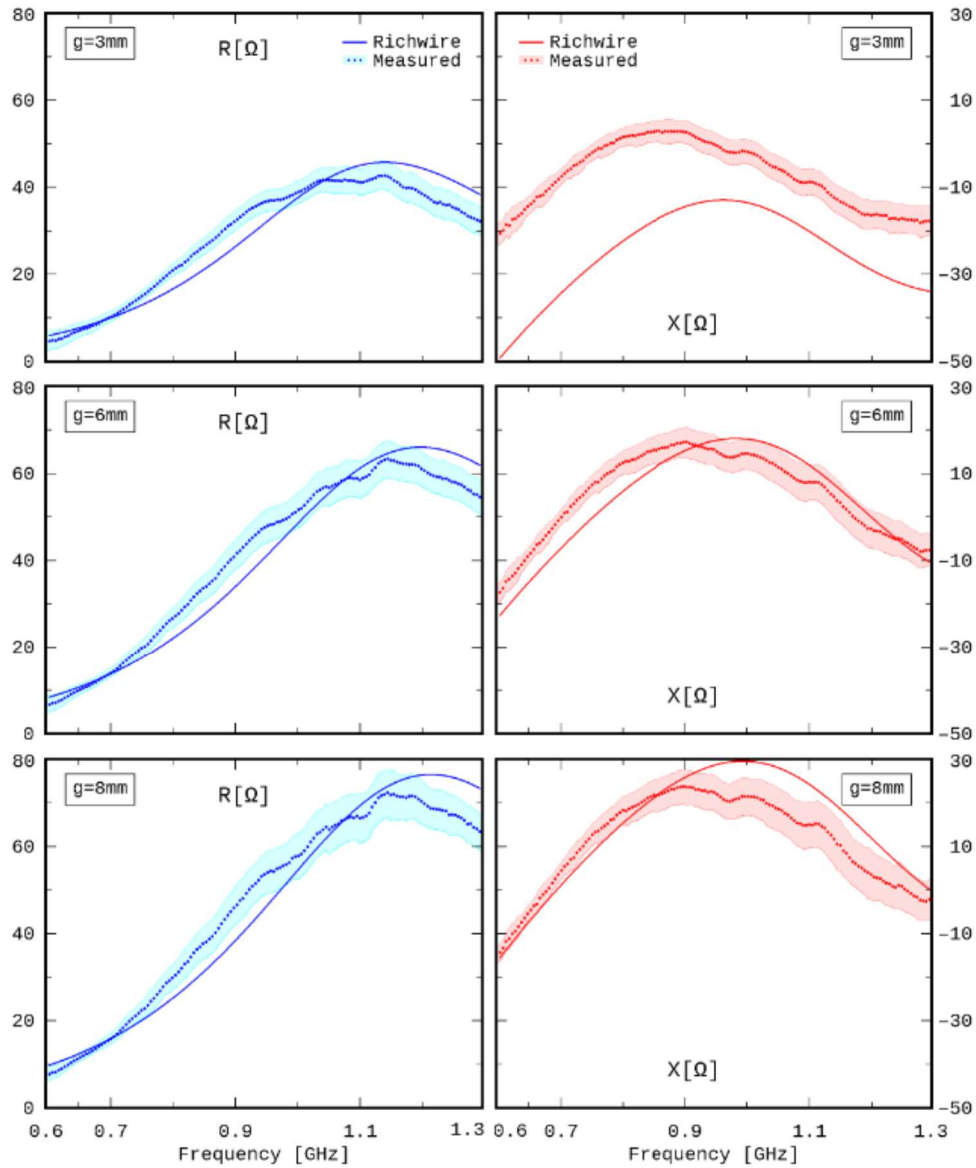
$a = 90^\circ$ ,  $D = 13.2$  cm,  $s = 12.5$  cm,  $d = 1.6$  cm


Fig. 29: Input impedance for B#1.1, B#1.2, B#1.3 models

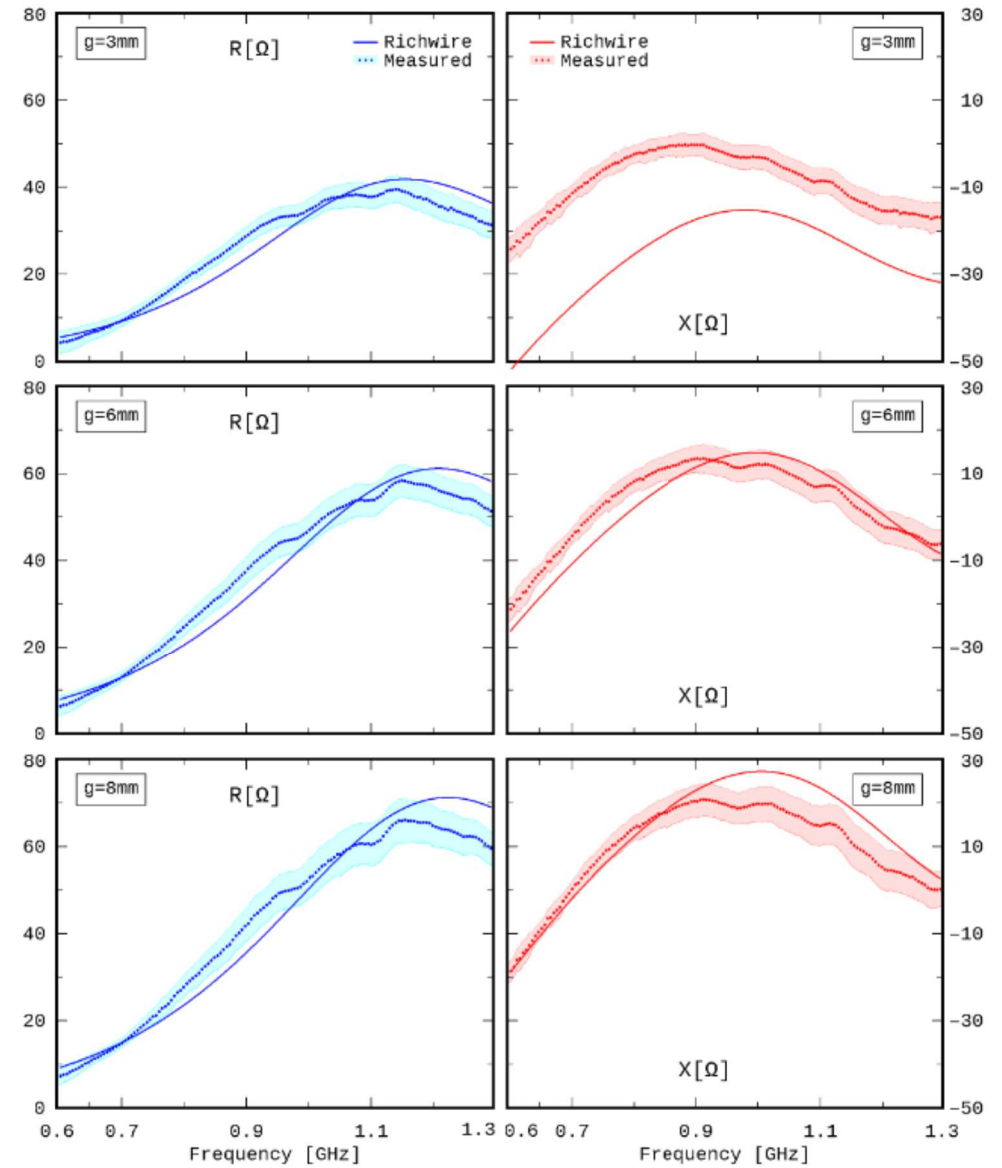
 $a = 90^\circ$ ,  $D = 12.4$  cm,  $s = 12.5$  cm,  $d = 1.6$  cm


Fig. 30: Input impedance for B#2.1, B#2.2, B#2.3 models

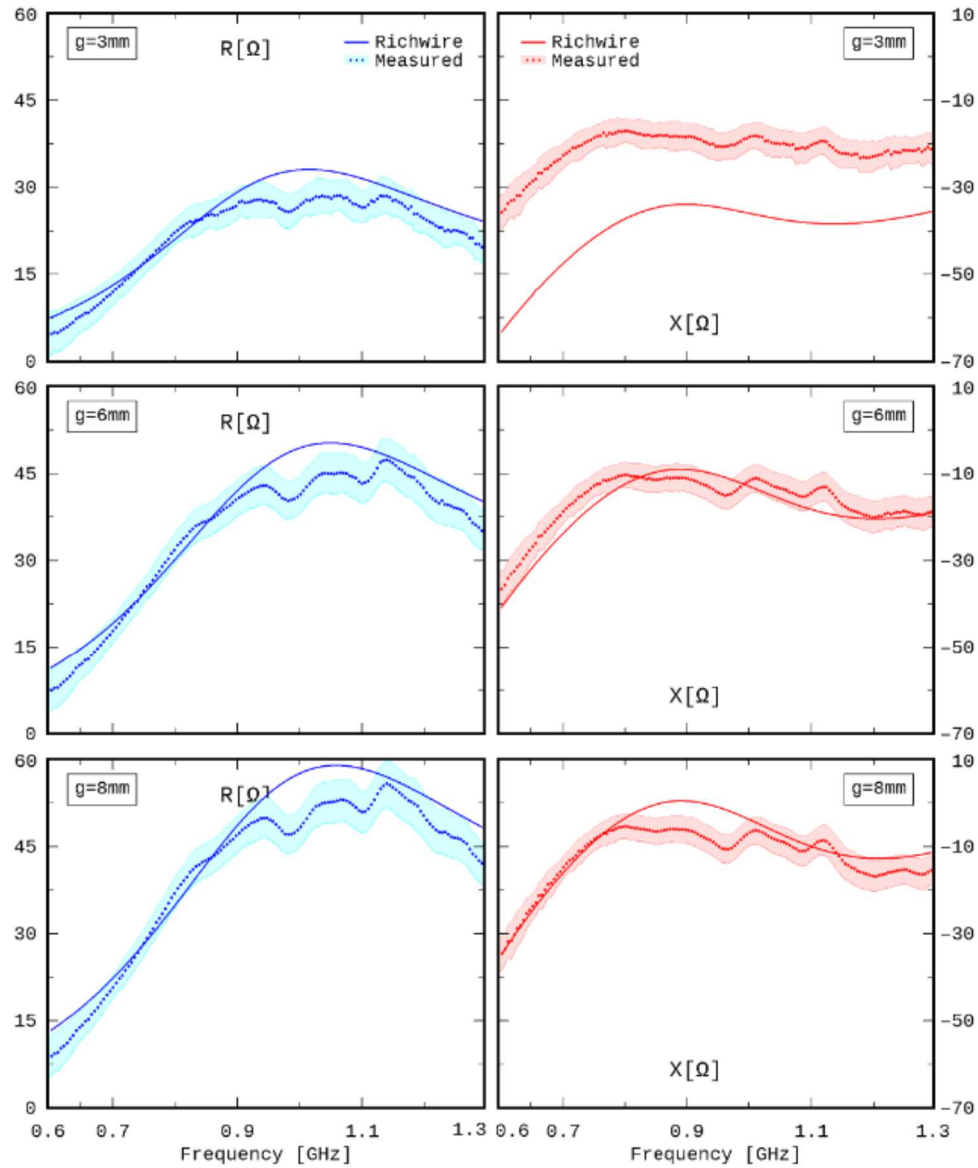
$a = 60^\circ$ ,  $D = 9.4$  cm,  $s = 12.5$  cm,  $d = 1.6$  cm


Fig. 31: Input impedance for C#1.1, C#1.2, C#1.3 models

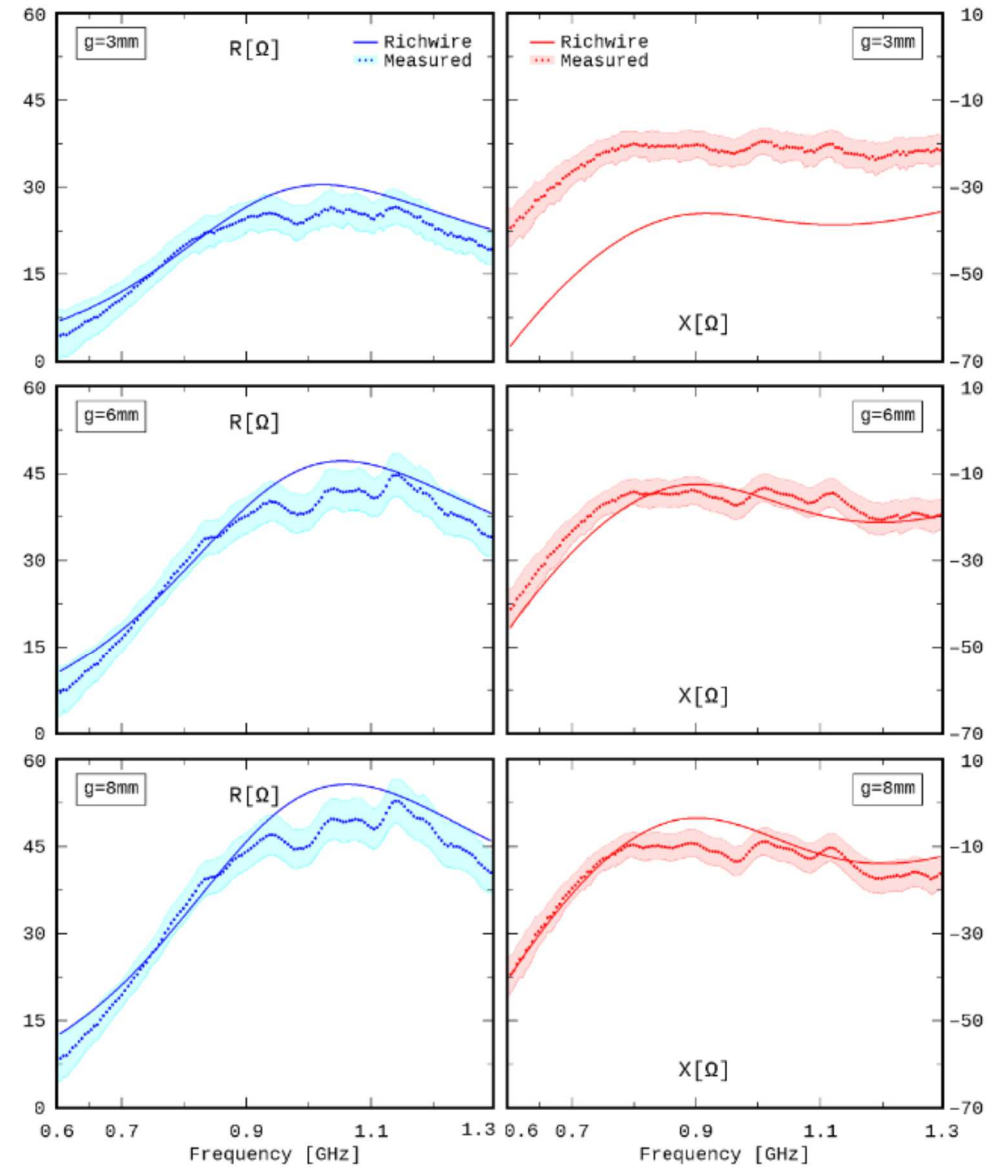
 $a = 60^\circ$ ,  $D = 8.8$  cm,  $s = 12.5$  cm,  $d = 1.6$  cm


Fig. 32: Input impedance for C#2.1, C#2.2, C#2.3 models

A#1.3, B#2.3, C#2.2 with (w) and without (w/o) line

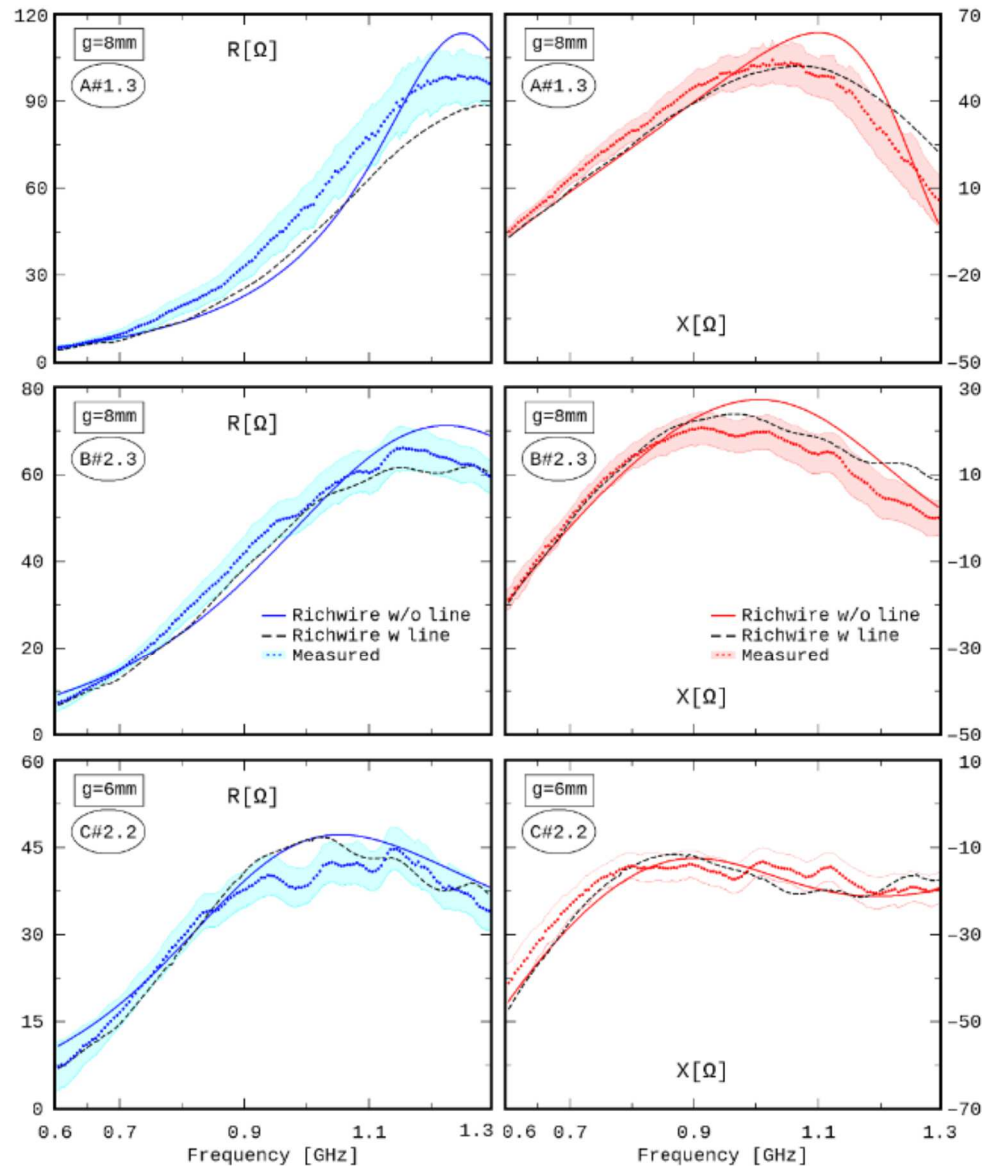
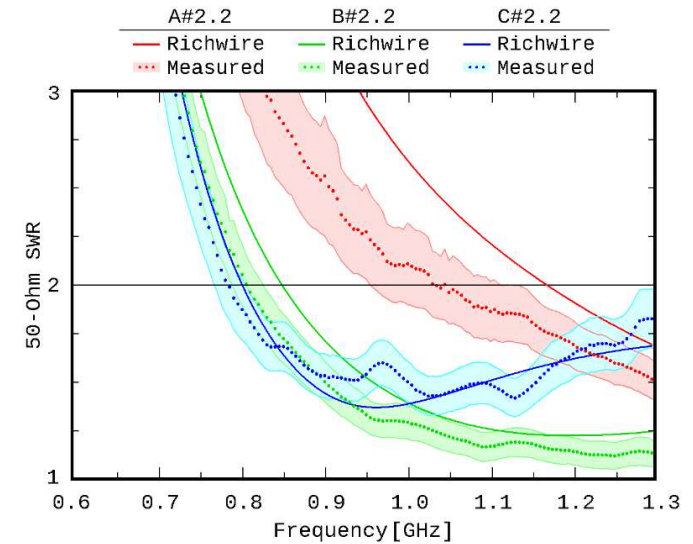


Fig. 33: Input impedance - Simulation with transmission line

Fig. 34: SWR:  $g = 6\text{ mm}$  - A#2.2:  $120^\circ$ , B#2.2:  $90^\circ$ , C#2.2:  $60^\circ$ 

### Conclusion

A detailed presentation of the study carried out for the radial discone antenna was given in [6], while in [1] the proposed antenna of [6], [11] was briefly presented. Here the analytical expression of the radiation pattern of a family of such antennas with 8 wires for both the disk and the cone was given. Two main construction difficulties were overcome with the methods described above: a) welding nine wires at one point, the center of the disk, and b) maintaining a constant cone angle. The radiation patterns for all the constructed antennas were presented. As already mentioned, and as expected, these patterns did

not differ between the 6 antennas of each category A ( $120^\circ$  cone angle), B ( $90^\circ$ ), and C ( $60^\circ$ ). Also presented here for the first time were the input impedance measurements of all fabricated antennas along with their DEIs, and the importance of adopting a simulation model that describes the antenna as closely as possible to its actual construction was demonstrated. An initial search was made for the impact or not of the inevitable transmission line, but without exhausting this issue. It was shown that Cooke's view [4] is more reliable at least for the radial discones. For all automated measurements, our program ANALYZE [15] was used

and all available software can be found in [16]. Finally, through SWR, one of the three criteria that gave the best antenna, C#2.2, ([5], [6], [11]), an optimism was achieved for the correctness of the predictions even for the frequency ranges where it is not yet possible to extend the measurements and a certainty for the adopted construction method as well as the adopted 3D model as the one that qualified as the most correct geometric simulation model.

### References

- [1] Kandoian A.G., "Three New Antenna Types and Their Applications", Proceedings of IRE, Vol. 34, February 1946, pp. 70W - 75W\*
- [2] Nail J.J., "Designing Discone Antennas", Electronics, August 1953, pp. 167 - 169
- [3] Rappaport T.S., "Discone Design Using N-Connector Feed", IEEE Antennas and Propagation Society Newsletter, Vol. 30, February 1988, pp. 12 - 14
- [4] Cooke D.W., "The Skeleton Discone", The ARRL Antenna Compendium, Vol. 3, 1993, pp. 140 - 143
- [5] Yannopoulou N.I., Zimourtopoulos P.E., Sarris E.T., "All-Band 2G+3G Radial Disc-Cone Antennas: Design, Construction and Measurements", FunkTechnikPlus # Journal, Issue 1, Year 1, 2013, pp. 7 - 15  
"https://www.ftpj.otoiser.org/issues/html/ftpj-issue-01-e4-lo4104-pdfc171-ia1.htm" (1-1)
- [6] Yannopoulou N.I., Zimourtopoulos P.E., "The Overall Antenna Bandwidth with an Application to the Improved Study of Radial Discone", FunkTechnikPlus # Journal, Issue 35, Year 12, 2024, pp. 25 - 48  
"https://www.ftpj.otoiser.org/issues/html/ftpj-issue-35-lo7532-export-ia1.htm" (35-2)
- [7] Richmond J.H., "Computer program for thin-wire structures in a homogeneous conducting medium", Publication Year: 1974, NTRS-Report/Patent Number: NASA-CR-2399, ESL-2902-12, DocumentID: 19740020595  
"https://ntrs.nasa.gov/search.jsp?R=19740020595"
- [8] Yannopoulou N., Zimourtopoulos P., "Total Differential Errors in One-Port Network Analyzer Measurements with Application to Antenna Impedance", Radioengineering, Vol. 16, No. 2, June 2007, p. 1 - 8  
"https://www.radioeng.cz/fulltexts/2007/07\_02\_01\_08.pdf"
- [9] Yannopoulou N., Zimourtopoulos P., "S-Parameter Uncertainties in Network Analyzer Measurements with Application to Antenna Patterns", Radioengineering, Vol. 17, No. 1, April 2008, pp. 1 - 8  
"https://www.radioeng.cz/fulltexts/2008/08\_01\_01\_08.pdf"
- [10] Zimourtopoulos P., "Antenna Notes 1999-, Antenna Design Notes 2000-(in Greek)  
"https://www.antennas.gr/antennanotes/"
- [11] Yannopoulou N.I., "Broadband Antenna Development for 3rd Generation Mobile Communication Systems", Master Thesis, EECE, DUTH, October 2003, (in Hellenic), Ch. 3  
"https://www.antennas.gr/theses/master/mt0-dc.pdf"  
"https://archive.org/details/discone-antenna-development-of-a-broadband-antenna-for-3rd-generation-mobile-telephony-systems"
- [12] Yannopoulou N.I., "Study of monopole antennas over a multi-frequency decoupling cylinder", PhD Thesis, EECE, DUTH, February 2008 (in Hellenic), pp. (2-6) - (2-9)  
"https://www.didaktorika.gr/eadd/handle/10442/20920?locale=en"
- [13] Yannopoulou N.I., Zimourtopoulos P., "Antenna Radiation Patterns: RadPat4W - FLOSS for MS Windows or Wine Linux", FunkTechnikPlus # Journal, Issue 5, Year 2, 2014, pp. 33 - 45  
"https://www.ftpj.otoiser.org/issues/html/ftpj-issue-05-lo4104-pdfc171-ia1.htm" (5-2)
- [14] Burberry R.A., "VHF and UHF Antennas", Peter Peregrinus Ltd., 1992, pp.129-137
- [15] Yannopoulou N., Zimourtopoulos P., "ANALYZE: Automated Antenna Measurements, ver. 13", Antennas Research Group, 1993-2008
- [16] Yannopoulou N., Zimourtopoulos P., "Radial Discone Antenna Software and Other Material - Current Versions",  
"https://updates.ftpj.otoiser.org/files/37-2"

\* Active Links: 31.05.2025 -  
Reference Updates : FTP#J Link :  
"https://updates.ftpj.otoiser.org/references/37-2"

---

This paper is licensed under a Creative Commons Attribution 4.0 International License - <https://creativecommons.org/licenses/by/4.0/>

[ This Page Intentionally Left Blank ]

In case of any doubt,  
download the genuine papers from  
<https://genuine.ftpj.otoiser.org>

## FRONT COVER VIGNETTE

A faded synthesis of an anthemion rooted in a meandros

The thirteen-leaf is a symbol for a life tree leaf.  
"Herakles and Kerberos", ca. 530–500 BC,  
by Paseas, the Kerberos Painter,  
Museum of Fine Arts, Boston.

[www.mfa.org/collections/object/plate-153852](http://www.mfa.org/collections/object/plate-153852)

The simple meandros is a symbol for eternal immortality.  
"Warrior with a phiale", ca. 480–460 BC,  
by Berliner Maler,  
Museo Archeologico Regionale "Antonio Salinas" di Palermo.

[commons.wikimedia.org/wiki/File:Warrior\\_MAR\\_Palermo\\_NI2134.jpg](https://commons.wikimedia.org/wiki/File:Warrior_MAR_Palermo_NI2134.jpg)

## ARG NfP AoI

Antennas Research Group  
Not-for-Profit Association of Individuals [\*]  
[www.arg.op4.eu](http://www.arg.op4.eu) – [arg@op4.eu](mailto:arg@op4.eu)  
Scheiblingkirchen, Austria

- \* The Constitution of Greece, Article 12(3) – 2008:  
[www.hellenicparliament.gr/en/Vouli-ton-Ellinon/To-Politevma](http://www.hellenicparliament.gr/en/Vouli-ton-Ellinon/To-Politevma)
- \* The Hellenic Supreme Court of Civil and Penal Law:  
[www.areiospagos.gr/en](http://www.areiospagos.gr/en) – Court Rulings:Civil|A1|511|2008